(0.5 mL) of the dispersion was then diluted with 3.0 mL isotonic borate buffer. The fluorescence intensities of these diluted suspensions were determined immediately. A total fluorescence value was determined by complete disruption of the vesicles, using 50 μL of a 80 mM Triton X-100 solution. Based on these measurements, a calibration curve was then constructed where the self-quenching efficiency was plotted as a function of the internal CF concentration. Self-quenching efficiency ($Q$) is defined as a percentage such that $Q$ (%) = $100[1 - (I/I_o)]$, where $I_o$ is the total fluorescence and $I$ is the fluorescence intensity of the entrapped CF.

In order to measure the internal volume of an osmotically-stressed vesicle, a 40-μL dispersion (10 mM in CF and 503 mosM in overall tonicity) was diluted with 2 mL of an appropriate buffer solution, followed by incubation for 0.5 h at 25 ± 1 °C. A portion (0.5 mL) was then added to 2.0 mL of this same buffer, and the self-quenching efficiency was determined from fluorescence intensity measurements before ($I$) and after ($I_o$) addition of excess Triton X-100. The concentration of intravesicular CF was then estimated by the use of an appropriate calibration curve.

**Stability of Osmotic Stress.** A 100-μL aliquot of the POPC/cholesterol (2/1) vesicles that were prepared for calibration measurements (10 mM CF and 503 mosM tonicity) was added to 5.0 mL of 10 mM borate buffer (269 mosM), and the mixture was incubated at 25 ± 1 °C. Aliquots (0.5 mL) were withdrawn as a function of time and were immediately chromatographed using a Sephadex G-50 column (0.7 × 15 cm). The vesicles (1.6 mL) were collected and added to 2.0 mL of 269 mosM normal borate buffer, and the fluorescence intensity of the mixture was analyzed to give a value for the vesicle-entrapped CF. A total fluorescence value was then measured after complete disruption of the vesicles, via addition of 50 μL of Triton X-100 (80 mM).

Aliquots (0.5 mL) were also withdrawn as a function of time and diluted with 3.0 mL of 10 mM, 269 mosM borate buffer, and their fluorescence was analyzed and compared with the above results. Self-quenching efficiency values showed that there were no significant differences from those found after gel filtration. These results indicate that the observed increase in fluorescence intensity is not the result of leakage of CF but is due to a dilution of the fluorophore that is entrapped within the vesicles.

This conclusion is also supported by osmotic reversibility studies. An aliquot (50 μL) of the 2.2 mM POPC/cholesterol (2/1) vesicle dispersion encapsulating 20 mM CF (269 mosM) was added to 2.0 mL of a 1 mM borate buffer (14 mM NaCl, 0.2 mM $NaN_3$, 36 mosM) and then incubated at 25 ± 1 °C. Aliquots (50 μL) were withdrawn as a function of time and diluted with 4.0 mL of same borate buffer, and their fluorescence was analyzed. At the same time, aliquots (50 μL) were also diluted with 4.0 mL of isotonic buffer in order to return the vesicles to an isotonic state, prior to analysis.

# Infrared Spectroscopic Study of the Photochemical Substitution and Oxidative Addition Reactions of $(\eta^5\text{-}C_5R_5)M(CO)_4$ Compounds of the Group 5 Metals: Characterization of the Products of Reaction with $N_2$, $H_2$, and $HSiEt_{3-x}Cl_x$ and the Kinetic Investigation of $(\eta^5\text{-}C_5R_5)M(CO)_3$ Intermediates

**Michael W. George,*,† Mark T. Haward,† Paul A. Hamley,† Catherine Hughes,† Frank P. A. Johnson,† Vladimir K. Popov,‡ and Martyn Poliakoff*,†**

*Contribution from the Department of Chemistry, University of Nottingham, Nottingham NG7 2RD, England, and LaserChem Laboratory, Scientific Centre for Technological Lasers, Troitzk, 142092 Moscow Region, Russia.* *Received June 2, 1992*

**Abstract:** IR spectroscopy has been used to study the photochemical reactions of $H_2$ and $N_2$ with $CpM(CO)_4$ and $Cp^*V(CO)_4$ ($Cp = \eta^5\text{-}C_5H_5$, $Cp^* = \eta^5\text{-}C_5Me_5$; M = V, Nb, and Ta) and of $HSiEt_{3-x}Cl_x$ ($x$ = 0, 2, and 3) with $CpV(CO)_4$. The reactions have been studied by FTIR in liquid xenon solution (lXe) at ca. −80 °C and by time-resolved IR spectroscopy (TRIR) in *n*-heptane solution at room temperature. In nearly all cases, UV irradiation leads to substitution of only *one* CO group. The only exceptions were the reactions of $N_2$ with $CpNb(CO)_4$ in lXe and with $CpV(CO)_4$ in solid matrices at 20 K, where $CpM(CO)_2(N_2)_2$ species were generated as secondary photoproducts. Reaction with $H_2$ led to formation of nonclassical dihydrogen complexes $CpV(CO)_3(\eta^2\text{-}H_2)$, $Cp^*V(CO)_3(\eta^2\text{-}H_2)$ and $CpNb(CO)_3(\eta^2\text{-}H_2)$, which was in thermal equilibrium with the classical dihydride $CpNb(CO)_3H_2$. $\nu$(H-H) IR bands have been observed for all three dihydrogen complexes. Reaction of $CpTa(CO)_4$ with $H_2$ led to oxidative addition and formation of $CpTa(CO)_3H_2$, which decayed over a period of 30 min in supercritical xenon solution at room temperature. IR data were also obtained for reaction with $D_2$ and, in the case of V, with HD. IR spectra suggest that reaction of $CpV(CO)_4$ with $HSiEt_3$ results in the arrested oxidative addition to form a labile $CpV(CO)_3(\eta^2\text{-}H\text{-}SiEt_3)$ complex, the first example of this type of compound of a group 5 metal. By contrast, reaction with $HSiCl_3$ and $HSiEtCl_2$ led to full oxidative addition, $CpV(CO)_3(H)SiR_3$. TRIR measurements showed that formation of all of these $CpM(CO)_3L$ species proceeds via a dissociative mechanism with transient formation of $CpM(CO)_3$. $CpV(CO)_3$ is ca. 100 times more reactive than its Nb and Ta analogs and nearly 1000 times more reactive than $CpMn(CO)_2$ under similar conditions. $Cp^*V(CO)_3$ is even more reactive. Photoacoustic calorimetry (PAC) has been combined with TRIR to estimate V-($N_2$) and V-($\eta^2$-$H_2$) bond dissociation enthalpies. The PAC results suggest that $CpV(CO)_3$ interacts with the *n*-heptane solvent and is probably more correctly formulated as $CpV(CO)_3\cdots$(*n*-heptane). Finally, the reactions of $V(CO)_6$ with $N_2$ and with $H_2$ were studied to compare the behavior of $d^5$ vanadium. IR evidence was found for the formation of $V(CO)_5(N_2)$ and $V(CO)_5(\eta^2\text{-}H_2)$ both in lXe and in *n*-heptane (TRIR). These compounds were significantly shorter lived than the corresponding $CpV(CO)_3L$ species under similar conditions. The photochemical formation of $V(CO)_5L$ occurred via $V(CO)_5$, detected by TRIR, which was significantly less reactive toward CO, $N_2$, and $H_2$ than was $CpV(CO)_3$.

## Introduction

The mechanism of oxidative addition of small molecules to transition metal centers has long been of interest.[1] Over recent years, whole new classes of compounds have been found where the oxidative addition is arrested and ligands are coordinated to

† University of Nottingham.
‡ Scientific Centre for Technological Lasers.

(1) See e.g.: Collman, J. P.; Hegedus, L. S.; Norton, J. R. *Principles and Applications of Organotransition Metal Chemistry*; University Science Books: Mill Valley, CA, 1987.

0002-7863/93/1515-2286$04.00/0 

the metal by three-center interactions; examples include agostic C–H bonds,[2] the $\eta^2$-H–$SiR_3$ coordination of silanes,[3] and the formation of "nonclassical" dihydrogen complexes.[4] As the number of new compounds grows, it is becoming increasingly clear that similar factors must influence the coordination of all of these ligands. The challenge, however, is to establish whether the relative importance of these factors (e.g. steric, electronic, geometric, etc.) is the same for different ligands and different metals.

The problem has been to find systems where these factors can be varied independently. Fragments of the type $(\eta^n\text{-}C_nR_n)M(CO)_2$ have proved particularly fruitful with the freedom to vary ring size, substituent, and the metal both down and across the Periodic Table (e.g. from Mn to Re or from Cr to Fe). In addition, there are several stable dinitrogen complexes[5] $[(\eta^n\text{-}C_nR_n)M(CO)_2(N_2)]$ where the $N_2$ group can be used as a model for other weakly interacting ligands. The $(\eta^n\text{-}C_nR_n)M(CO)_2$ fragments have usually been generated photochemically from the corresponding tricarbonyl complex[3] (eq 1). Such reactions have been carried out

$$(\eta^n\text{-}C_nR_n)M(CO)_3 \xrightarrow{UV} (\eta^n\text{-}C_nR_n)M(CO)_2 + CO \xrightarrow{L} (\eta^n\text{-}C_nR_n)M(CO)_2L \quad (1)$$

under conditions ranging from hydrocarbon glasses[6] to supercritical fluids,[7] and the $(\eta^n\text{-}C_nR_n)M(CO)_2L$ products have been investigated by a plethora of structural and spectroscopic techniques.[3] The kinetics have been probed by transient spectroscopy[8] and the energetics by photoacoustic calorimetry.[9] The limitation, however, is that all of these metal centers have a $d^6$ electron configuration. Indeed, the majority of nonclassical dihydrogen[4] and $\eta^2$-H–$SiR_3$ complexes[3] have involved $d^6$ centers, and it is important to determine how metal centers with other d electron configurations behave.[10]

This paper is aimed at exploring the interaction of small molecules with $CpM(CO)_3$ (Cp = $\eta^5$-$C_5H_5$; M = V, Nb, and Ta) and related species which incorporate a $d^4$ metal center yet retain sufficient similarity to the analogous $CpM(CO)_2$ species (M = Mn and Re) for direct comparisons to be fruitful. Our strategy has been to study the photochemical reactions of these compounds with $H_2$, $N_2$, and silanes.

Although the products of these reactions have proved to be thermally far more labile than the corresponding group 6 and 7 compounds, we show below that it is possible not only to characterize them by IR spectroscopy but also to study the kinetics of their formation in some detail.

The photochemistry of $CpV(CO)_4$ is relatively unexplored compared to that of $CpMn(CO)_3$. Nevertheless, the ease of photoejection of CO from $CpV(CO)_4$ and the subsequent substitution of CO by various ligands is well documented.[11] The photochemistries of $CpNb(CO)_4$ and $CpTa(CO)_4$ have been studied much less than that of $CpV(CO)_4$, possibly because these compounds do not appear to be available commercially. Unlike the group 6 and 7 systems, stable $CpM(CO)_x(N_2)$ complexes are not known for the group 5 metals. However, Rest and co-workers have found IR evidence[14] for the formation of dinitrogen compounds ($CpV(CO)_3(N_2)$, etc.) generated by photochemical reaction of $CpV(CO)_4$ and its $C_5Me_5$ analog in solid $N_2$ matrices at 12 K. Such experiments cannot, of course, provide any indication of the thermal stability of these complexes because, on heating, the matrix evaporates almost immediately (ca. 30 K) well below the likely decomposition temperature of such species.[15] Recently, we reported preliminary experiments[16] showing that UV photolysis of $CpV(CO)_4$ in ligand xenon solution (lXe) doped with $N_2$ led to the formation of $CpV(CO)_3(N_2)$, the IR spectrum of which agreed broadly with Rest's matrix results.[14a]

It is much more difficult to use $H_2$ than $N_2$ in matrix isolation experiments[10b] because of the very low boiling point of $H_2$, and there are, therefore, no matrix data for the reaction of $CpV(CO)_4$ with $H_2$. However, UV photolysis of $CpV(CO)_4$ and $H_2$ in lXe resulted in the formation of $CpV(CO)_3(\eta^2\text{-}H_2)$, the first nonclassical dihydrogen complex of vanadium,[16] characterized by a weak IR band (2640 $cm^{-1}$) due to the $\nu$(H–H) vibration of $\eta^2$-$H_2$. The complete IR transparency of lXe was vital in this experiment, because the $\nu$(H–H) band would have been masked by the IR absorption bands of conventional hydrocarbon solvents. $CpV(CO)_3(\eta^2\text{-}H\text{-}D)$ was generated by repeating the photolysis in the presence of HD rather than $H_2$, and the observation of the $\nu$(H–D) band (2380 $cm^{-1}$) provided particularly striking proof of $\eta^2$-coordination of HD (1), since the presence of such a band cannot

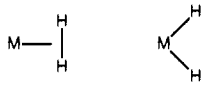

1 2

be explained on the basis of the classical species (2). Time-resolved IR spectroscopy (TRIR),[18] a combination of UV flash photolysis and very fast IR spectroscopy (see Experimental Section) has shown that photolysis of $CpV(CO)_4$ and $H_2$ in *n*-heptane solution at room temperature also leads to formation[17] of $CpV(CO)_3$-

(2) For a recent review on agostic interactions, see: Brookhart, M.; Green, M. L. H.; Wong, L. L. *Prog. Inorg. Chem.* **1988**, *36*, 1.

(3) For a recent review on silane complexes, see: Schubert, U. *Adv. Organomet. Chem.* **1990**, *30*, 151.

(4) For recent reviews on dihydrogen complexes, see e.g.: Kubas, G. J. *Acc. Chem. Res.* **1988**, *21*, 120. Crabtree, R. H.; Hamilton, D. G. *Adv. Organomet. Chem.* **1989**, *28*, 299. Ginsburg, A. G.; Bagaturyants, A. A. *Organomet. Chem. USSR* **1989**, *2*, 111.

(5) See, e.g.: Sellmann, D. *Angew. Chem., Int. Ed. Engl.* **1971**, *10*, 919.

(6) Black, J. D.; Boylan, M. J.; Braterman, P. S. *J. Chem. Soc., Dalton Trans.* **1981**, 673. Hill, R. S.; Wrighton, M. S. *Organometallics*, **1987**, *6*, 632.

(7) Howdle, S. M.; Poliakoff, M.; Healy, M. A. *J. Am. Chem. Soc.* **1990**, *112*, 4804.

(8) (a) Creaven, B. S.; Dixon, A. J.; Kelly, J. M.; Long, C.; Poliakoff, M. *Organometallics* **1987**, *6*, 2600. (b) Johnson, F. P. A.; George, M. W.; Bagratashvili, V. N.; Vereshchagina, L. N.; Poliakoff, M. *Mendeleev Commun.* **1991**, 26.

(9) Klassen, J. K.; Selke, M.; Sorensen, A. A.; Yang, G. K. *J. Am. Chem. Soc.* **1990**, *112*, 1267.

(10) A few examples of dihydrogen complexes for other *d* electron configurations have been found in low-temperature experiments, e.g. (a) $d^{11}$ $Fe(CO)(NO)_2(\eta^2\text{-}H_2)$ in lXe (Gadd, G. E.; Upmacis, R. K.; Poliakoff, M.; Turner, J. J. *J. Am. Chem. Soc.* **1986**, *108*, 2547) and (b) $d^4$ $CpMo(CO)_2H(\eta^2\text{-}H_2)$ in solid noble gas matrices at 10 K (Sweany, R. L. *J. Am. Chem. Soc.* **1986**, *108*, 6986).

(11) For a general review, see Srivastava, S. C.; Shrimal, A. K. *Polyhedron* **1988**, *7*, 1639. Photolysis of $CpV(CO)_4$ in the presence of phosphines and similar ligands, L, leads to production of monosubstituted complexes[12] ($CpV(CO)_3L$). Photoreactions with bidentate phosphines, L–L (e.g. $PhP(CH_2)_nPPh_2$; *n* = 1, 2, or 4), have been reported to give disubstituted products[13a] ($CpV(CO)_2(L\text{–}L)$). Alkyne complexes have also been prepared by photolysis of $CpV(CO)_4$ in the presence of a variety of alkynes[13b] ($RC{\equiv}CR'$).

(12) (a) L = $PPh_3$: Tsumura, R.; Hagihara, N. *Bull. Chem. Soc. Jpn.* **1965**, *38*, 1901. Kinney, R. J.; Jones, W. D.; Bergman, R. G. *J. Am. Chem. Soc.* **1978**, *100*, 7902. Alway, D. G.; Barnett, K. W. *Inorg. Chem.* **1980**, *19*, 779. (b) L = $PH_3$ or $P(n\text{-}Bu)_3$: Fischer, E. O.; Schneider, R. J. J. *Angew. Chem., Int. Ed. Engl.* **1967**, *6*, 569. (c) L = $P(n\text{-}Bu)_3$: Fischer, E. O.; Louis, E.; Schneider, R. J. *J. Angew. Chem., Int. Ed. Engl.* **1968**, *7*, 136. (d) L = diene: Wrighton, M. S. *Chem. Rev.* **1974**, *74*, 401. (e) L = $EMe_2$ (E = S or Te): Belforte, A.; Calderazzo, F.; Zanazzi, P. F. *Gazz. Chim. Ital.* **1985**, *17*, 115. (f) L = THF: Fischer, E. O.; Schneider, R. J. J. *Chem. Ber.* **1970**, *103*, 3684. Hoch, M.; Rehder, D. *J. Organomet. Chem.* **1985**, *288*, C25. Huffman, J. C.; Lewis, L. N.; Caulton, K. G. *Inorg. Chem.* **1980**, *19*, 2755. Cotton, F. A.; Kruczynsky, L.; Frenz, B. A. *J. Organomet. Chem.* **1978**, *93*, 160.

(13) (a) Rehder, D.; Dahlenburg, L.; Mueller, I. *J. Organomet. Chem.* **1976**, *122*, 53. (b) Foust, D. F.; Rausch, M. D. *J. Organomet. Chem.* **1982**, *239*, 321. Alt, H. G.; Engelhardt, H. E. *Z. Naturforsch.* **1985**, *40B*, 1134.

(14) (a) Hitam, R. B.; Rest, A. J. *Organometallics* **1989**, *8*, 1598. (b) Rest, A. J.; Herberhold, M.; Schrepfermann, M. *Organometallics* **1992**, *11*, 3646.

(15) See, for example: Almond, M. J.; Downs, A. J. Spectroscopy of Matrix Isolated Species. *Adv. Spectrosc.* **1989**, *17*, 1.

(16) Haward, M. T.; George, M. W.; Howdle, S. M.; Poliakoff, M. *J. Chem. Soc., Chem. Commun.* **1990**, 913.

(17) Under these conditions, $CpV(CO)_3(\eta^2\text{-}H_2)$ is considerably shorter lived (i.e. 20 ms under 2 atm of $H_2$) than in lXe. It probably reacts by dissociative loss of $H_2$, since its lifetime can be extended by increasing the pressure of $H_2$.

(18) (a) Poliakoff, M.; Weitz, E. *Adv. Organomet. Chem.* **1986**, *25*, 277. (b) Grevels, F.-W.; Klotzbücher, W. E.; Schaffner, K. *Chem. Rev.*, in press.

($\eta^2$-$H_2$). Faster TRIR measurements showed that $CpV(CO)_3$-($\eta^2$-$H_2$) is formed extremely rapidly, within 1 μs of the UV flash.[19]

By contrast, UV photolysis of $CpTa(CO)_4$ with $H_2$ in lXe solution produced IR evidence[20] for the formation of the classical dihydride $CpTa(CO)_3H_2$. Although the change from nonclassical dihydrogen complex to dihydride between first- and third-row metals has already been observed in other groups of the Periodic Table,[4] it is the behavior of Nb which makes group 5 particularly interesting. UV photolysis of $CpNb(CO)_4$ and $H_2$ in both lXe and *n*-heptane generates a *mixture* of the classical $CpNb(CO)_3H_2$ and nonclassical $CpNb(CO)_3(\eta^2\text{-}H_2)$ complexes, easily identifiable by the similarity of their IR spectra to the corresponding Ta and V compounds.[20] The two Nb compounds are in thermodynamic equilibrium, and as the temperature is raised, the proportion of $CpNb(CO)_3H_2$ grows reversibly at the expense of $CpNb(CO)_3$-($\eta^2$-$H_2$) (eq 2). The value of $\Delta H°$ (−3.5 kJ mol$^{-1}$; −5.5 kJ mol$^{-1}$ for $D_2$) indicates just how delicate is the balance between "arrested" and full oxidative addition of $H_2$ in this case. TRIR measurements at room temperature showed that the rate of equilibrium between $CpNb(CO)_3H_2$ and $CpNb(CO)_3(\eta^2\text{-}H_2)$ was fast, probably occurring on a submicrosecond time scale.[20] The speed of this interconversion contrasts strongly with those of most previously reported cases of hydride ⇌ dihydrogen interconversion, which were sufficiently slow to be followed by NMR techniques.[4]

$$CpNb(CO)_3(\eta^2\text{-}H_2) \rightleftarrows CpNb(CO)_3H_2 \qquad (2)$$

Our present study aims to expand our preliminary results[16,19,20] and to establish a basis for discussing oxidative addition in these systems. The first part of this paper is primarily concerned with the characterization of the coordinatively saturated $CpM(CO)_3L$ photoproducts in lXe by FTIR and in *n*-heptane solution at room temperature by TRIR. The second part reports TRIR data for the transient formation of the "unsaturated" intermediate $CpM(CO)_3$, the kinetics of the formation of $CpM(CO)_3L$ at room temperature, and a study of the energetics of these processes using photoacoustic calorimetry. The behavior of $V(CO)_6$ is then compared with that of $CpV(CO)_4$ under similar conditions.

## Experimental Section

**(a) Matrix Isolation and Liquid Xenon.** Our equipment for matrix isolation (Air Products CS-202 Displex)[21] and for lXe experiments (miniature Cu cell cooled with liquid $N_2$)[22] have been described previously. Matrices were deposited by slow deposition with $N_2$ (Messer-Griesheim) or Ar (BOC research grade). FTIR spectra were recorded with Nicolet interferometers: for matrix isolation, MX3600 interferometer with Model 1280 data station, 32K data points (0.7 cm$^{-1}$ resolution), 256K transform points, "Box car" apodization; for lXe, Model 730 interferometer with MCT detector and 620 or 680 data stations, 16K data points (2 cm$^{-1}$), 32K transform points, Happ–Genzel apodization. The UV photolysis sources were a Philips HPK 125-W medium-pressure Hg arc and a Cermax 300-W Xe arc with a 1 m long Lumatec liquid lightguide, an innovation which almost completely eliminates the hazard of scattered UV light in the experiments. In every case, experiments were carried out with irradiation of $CpM(CO)_4$ *in the absence of* added ligands. The results of these "blank" experiments are only reported in detail where significant changes in the IR spectra were observed.

**(b) Time-Resolved IR Spectroscopy (TRIR).** The Nottingham TRIR equipment has also been described before.[23] Briefly, it consists of a XeCl UV excimer laser (308 nm and 20-ns pulse, Lumonics HyperEx 440) to initiate photochemical reactions and a tunable CW IR laser to monitor the transient IR absorptions. IR spectra are built up on a "point-by-point" basis. The work described here has involved two different monitoring lasers, an Edinburgh Instruments Model PL3 CO laser, line tunable in steps of ca. 4 cm$^{-1}$ over a limited wavenumber range, and a Mütek IR diode laser (Model MDS 1100, fitted with a Mütek Model MDS 1200 monochromator), which has much lower power but is continuously tunable so that higher resolution TRIR spectra can be obtained. The problems of lower power can be at least partly offset by careful design of the optical layout.[24] Continuous tunability, however, introduces the need for rather more precise calibration of the wavenumber of the IR monitoring beam. In the experiments described here, we achieved this calibration by diverting the IR beam into a high-resolution (0.06 cm$^{-1}$) FTIR interferometer (Nicolet Model 7199) as shown in Figure 1. Two different detectors were used for the CO laser experiments, the first (HgCdTe photoconductive, New England Research Center MPC4) with ca. 1-μs response and the other substantially faster (150 ns, HgCdTe photovoltaic Laser Monitoring Systems S-025). Diode laser signals were detected with a HgCdTe detector (New England Research Center MPC4.5-1.0-B12 with 1-μs risetime). Signals were digitized with Datalab Model 902 (1-MHz) or Gould Model 4052 (100-MHz) digitizers.

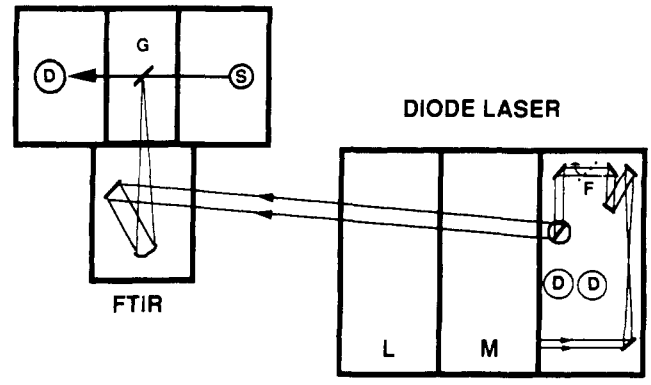


**Figure 1.** Schematic optical diagram, showing the arrangement for FTIR calibration of the IR diode laser in TRIR experiments. The Mütek IR diode laser spectrometer, shown schematically on the right-hand side of the figure, consists of three modules: Laser, L, Monochromator, M, and Optics. In normal operation, the spectrometer has two detectors, marked D, and the IR beam is switched between them with a manually operated "flip" mirror, F. For TRIR, we use only one detector and a simple periscope is placed in front of the other detector. The flip mirror can then be used to divert the IR beam, via the periscope, into the FTIR interferometer, shown on the left of the figure. The beam is focussed onto a Ge beam splitter, G, oriented at 45° to the optic axis of the interferometer in the FTIR sample compartment. IR emission spectra of the laser are then obtained by operating the FTIR normally but with the conventional IR source, S, switched off. Interferograms are undersampled with 131K data points and 256K transform points to give 0.06-cm$^{-1}$ resolution. With an InSb detector, D, in the interferometer, only a few scans (<20) are needed to get an excellent S/N ratio. An FTIR spectrum of the laser output serves two purposes, (i) to check that the laser emission consists of a single wavelength (if more than one line is detected, the laser is adjusted accordingly) and (ii) to measure this wavelength precisely. After measurement, the wavenumber of the laser output is entered manually into the computer programs for plotting TRIR spectra.

**(c) Photoacoustic Calorimetry (PAC).** Experimental details of our photoacoustic apparatus have been published recently.[19] The PAC cell was built at the Scientific Centre for Technological Lasers in Troitzk (Moscow), and the experiments were carried out in Nottingham. The UV laser, digitizers, etc. were the same as those for TRIR. Our PAC cell gave acceptable agreement with published enthalpy measurements[9] (e.g. with $CpMn(CO)_3$). All PAC measurements were made using reaction and reference solutions with very similar absorbance values (±5%) at 308 nm, as measured on a Perkin-Elmer Lambda 5 spectrometer. Readings were normalized for laser pulse energy and minor differences in absorbance. Fresh reference measurements were made for each reactant (i.e. under pressures of Ar, CO, $H_2$, and $N_2$). Each measurement was made "single shot" and was repeated ca. 25 times to obtain a mean value, and each experiment was itself repeated several times.

**(d) Chemicals.** Carbonyl compounds were obtained as follows: $CpV(CO)_4$, Strem, sublimed before use; $Cp^*V(CO)_4$, gift from Prof. M. Herberhold; $CpNb(CO)_4$ and $CpTa(CO)_4$, gifts from Prof. F. Basolo.

(19) Johnson, F. P. A.; Popov, V. K.; George, M. W.; Bagratashvili, V. N.; Poliakoff, M.; Turner, J. J. *Mendeleev Commun.* **1991**, 145.

(20) Haward, M. T.; George, M. W.; Hamley, P. A.; Poliakoff, M. *J. Chem. Soc., Chem. Commun.* **1991**, 1101.

(21) For recent descriptions, see: Gordon, C. M. Ph.D. Thesis, University of Nottingham, 1992. Johnson, F. P. A.; Gordon, C. M.; Hodges, P. M.; Poliakoff, M.; Turner, J. J. *J. Chem. Soc., Dalton Trans.* **1991**, 833.

(22) (a) Turner, J. J.; Poliakoff, M.; Howdle, S. M.; Jackson, S. A.; McLaughlin, J. G. *Faraday Discuss. Chem. Soc.* **1988**, *86*, 271 and references therein. (b) Haward, M. T. Ph.D. Thesis, University of Nottingham, 1991.

(23) (a) Dixon, A. J.; Healy, M. A.; Hodges, P. M.; Moore, B. D.; Poliakoff, M.; Simpson, M. B.; Turner, J. J.; West, M. A. *J. Chem. Soc., Faraday Trans. 2* **1986**, *82*, 2083. (b) George, M. W. Ph.D. Thesis, University of Nottingham, 1990.

(24) Howdle, S. M.; Jobling, M.; George, M. W.; Poliakoff, M. In *Proceedings of the 2nd International Symposium on Supercritical Fluids (Boston)*; McHugh, M. A., Ed.; Johns Hopkins University, 1991; p 189.

**Table I.** Wavenumbers ($cm^{-1}$) of $CpM(CO)_{4-x}(N_2)_x$ Species (M = V, Nb, and Ta) in Liquid Xenon Solution (lXe) at ca. −70 °C, in *n*-Heptane Solution at Room Temperature, and in Cryogenic Matrices

| species | lXe[a] | *n*-heptane[b] | matrix[a,c] | assignment |
|---|---|---|---|---|
| $CpV(CO)_4$ | 2032.3 [2021][e] | 2029.4[a] | 2032.3 | $a_1$ $\nu$(C–O) |
| | 1934.1 [1930][e] | 1931.8[a] | 1938.4/32.5 | e $\nu$(C–O) |
| $CpV(CO)_3(N_2)$ | 2199.5 [2163.8][d] | | 2216.9/08.3 | $\nu$(N–N) |
| | 1995.2 [1987.6][e] | 1997 | 1995.2 | a′ $\nu$(C–O) |
| | 1915.5 | 1916 | 1912.7 | a′ $\nu$(C–O) |
| | 1911.4 [1878.2][e] | 1908 | 1909.8 | a″ $\nu$(C–O) |
| $CpV(CO)_2(N_2)_2$ | | | 2203.8 | $\nu$(N–N) |
| | | | 2171.8 | $\nu$(N–N) |
| | | | 1876.3 | $\nu$(C–O) |
| $Cp^*V(CO)_4$ | 2016.5 | 2014.9[a] | | $a_1$ $\nu$(C–O) |
| | 1919.1 | 1917.0[a] | | e $\nu$(C–O) |
| $Cp^*V(CO)_3(N_2)$ | 2180.9 | | 2192[f] | $\nu$(N–N) |
| | 1978.1 | 1980 | 1981[f] | a′ $\nu$(C–O) |
| | 1899.6 | 1900 | 1900[f] | a′ $\nu$(C–O) |
| | 1887.1 | 1900 | | a″ $\nu$(C–O) |
| $CpNb(CO)_4$ | 2038.5 | 2037.0[a] | | $a_1$ $\nu$(C–O) |
| | 1933.5 | 1931.9[a] | | e $\nu$(C–O) |
| $CpNb(CO)_3(N_2)$ | 2193 | | | $\nu$(N–N) |
| | 1992.5 | 1993 | | a′ $\nu$(C–O) |
| | 1906.2 | 1903 | | a′ + a″ $\nu$(C–O) |
| $CpNb(CO)_2(N_2)_2$ | 2180 | | | $\nu$(N–N) |
| | 2141 | | | $\nu$(N–N) |
| | 1873 | | | a″ $\nu$(C–O) |
| $CpTa(CO)_4$ | 2036.0 [2027][d] | 2033.5[a] | 2038.1[g] | $a_1$ $\nu$(C–O) |
| | 1925.6 [1892.6][d] | 1923.0[a] | 1930.6/26.6[g] | e $\nu$(C–O) |
| $CpTa(CO)_3(N_2)$ | 2164 | | 2170[g] (br) | $\nu$(N–N) |
| | 1985.8 [1973][d] | 1987 | | a′ $\nu$(C–O) |
| | 1899.1 [1894][d] | 1903 | 1906/1900[g] | a′ + a″ $\nu$(C–O) |

[a] FTIR, ±0.2 $cm^{-1}$. [b] CO laser TRIR, ±2 $cm^{-1}$. [c] $N_2$ matrix, 20 K, this work. [d] Natural abundance $^{15}N^{14}N$ satellite. [e] Natural abundance $^{13}CO$ satellites. [f] $N_2$ matrix, ref 14b. [g] Ar matrix doped with $N_2$.

$V(CO)_6$ was prepared by reaction[25] of excess $H_3PO_4$ with $Na[V(CO)_6]$ and sublimation of $V(CO)_6$ directly into the lXe cell or reservoir of the TRIR flow cell. The concentration of $V(CO)_6$ in lXe or *n*-heptane was then estimated from the absorbance of the $\nu$(C–O) IR bands. $HSiEt_3$, $HSiEtCl_2$, and $HSiCl_3$ (Aldrich) were redistilled before use. For lXe experiments, Xe, $H_2$, $N_2$ (BOC research grade), $D_2$ (BDH), and HD (MSD Isotopes) were used without further purification. For TRIR experiments: *n*-heptane (HPLC grade) was distilled over $CaH_2$; Ar, $H_2$, $D_2$, $N_2$ (Messer-Griesheim), and CO (BOC research grade) were used as supplied; and unless otherwise stated, the concentrations of carbonyl compounds in *n*-heptane were $7 \times 10^{-4}$ M for $CpV(CO)_4$, $Cp^*V(CO)_4$, and $CpNb(CO)_4$ and $4 \times 10^{-4}$ M for $CpTa(CO)_4$. All TRIR experiments were carried out at 25 ± 2 °C, unless otherwise stated.

## Results and Discussion

**1. Characterization of the Reaction Products. (a) Reaction of $CpV(CO)_4$ with $N_2$.** The four CO groups in $CpV(CO)_4$ have local $C_{4v}$ symmetry (**3**), and the molecule shows the expected two IR active $\nu$(C–O) vibrations ($a_1$ + e). Substitution of one CO group by a ligand L (e.g. $N_2$) reduces the symmetry of the $V(CO)_3$ moiety to $C_s$ (**4**), with *three* IR active $\nu$(C–O) vibrations (2a′ + a″).

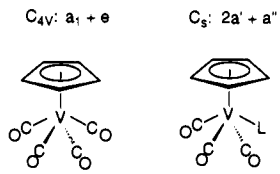


3 4

Figure 2b shows the IR spectrum of $CpV(CO)_3(N_2)$ generated by photolysis of $CpV(CO)_4$ and $N_2$ in lXe. Two of the expected three $\nu$(C–O) bands are easily recognized. In more concentrated solutions, one can detect two very weak satellite bands due to natural abundance $^{13}CO$ (Table I). The wavenumbers of these four bands provide sufficient data to calculate the four energy factored force constants of the $V(CO)_3$ moiety (two C–O stretching and two interaction constants, see Table IVB). These

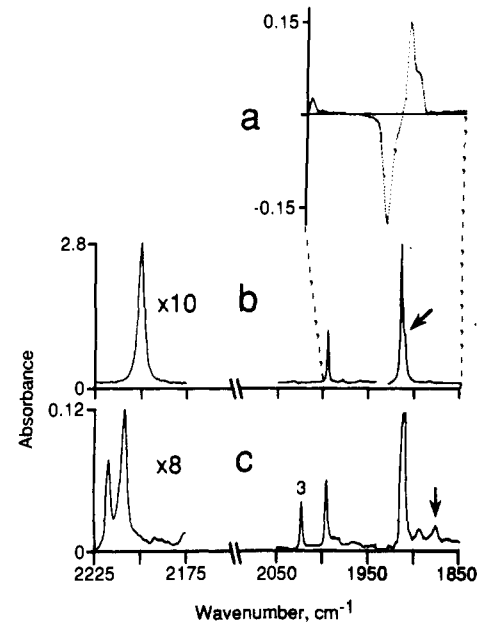


**Figure 2.** IR spectra obtained after UV photolysis of $CpV(CO)_4$ in the presence of $N_2$, illustrating the formation of $CpV(CO)_3(N_2)$. (a) CO laser TRIR difference spectrum in *n*-heptane under 2 atm of $N_2$ at room temperature, corresponding to a time of 10 $\mu$s after the UV flash. The positive bands are due to $\nu$(C–O) vibrations of $CpV(CO)_3(N_2)$, and the negative band is due to the e mode of $CpV(CO)_4$ destroyed. (Note that the tuning range of the CO laser restricts the wavenumber range of the spectrum). (b) FTIR spectrum obtained after UV photolysis ($\lambda > 300$ nm) in lXe doped with ca. 170 psi of $N_2$ at −70 °C. The arrow indicates the position of the third $\nu$(C–O) band of $CpV(CO)_3(N_2)$, which is not fully resolved under these conditions. (c) FTIR spectrum recorded after 12-min photolysis ($\lambda > 450$ nm) of $CpV(CO)_4$ in solid $N_2$ at 20 K. The unlabeled bands are assigned to $CpV(CO)_3(N_2)$; the band marked 3 has been assigned[14a] to a product with an $\eta^3$-$C_5H_5$ ring; and the arrow indicates the band previously attributed[14a] to $CpV(CO)_3(N_2)$ but reassigned in this paper. Note that, in both parts b and c, the $\nu$(N–N) regions are shown with expanded absorbance scales and that the $\nu$(C–O) bands of $CpV(CO)_4$ have been removed by computer subtraction.

(25) Silvestri, G.; Gambino, S.; Guainzari, M.; Ercoli, R. *J. Chem. Soc., Dalton Trans.* **1972**, 2558.

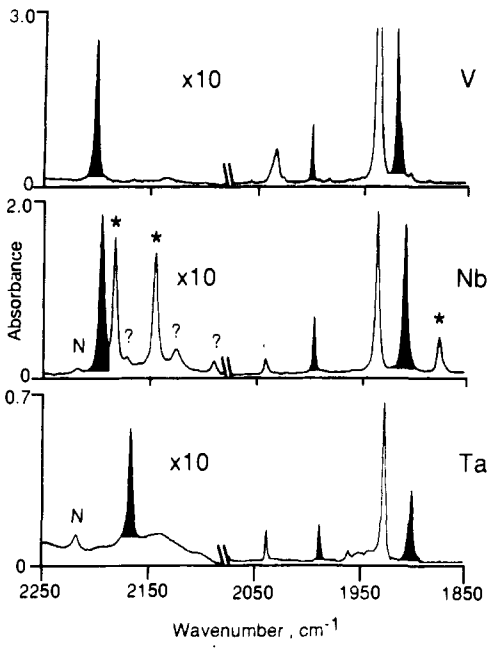


Figure 3. FTIR spectra comparing the results of UV photolysis ($\lambda > 300$ nm) of $CpM(CO)_4$ (M = V, Nb, and Ta) in lXe doped with 150 psi of $N_2$ at −70 °C. Bands are identified as follows: unlabeled, $CpM(CO)_4$; colored, $CpM(CO)_3(N_2)$; *, $CpNb(CO)_2(N_2)_2$; ?, $CpNb(CO)(N_2)_3$ (tentative assignment); N, $N_2O$, probably generated by reaction with trace impurities of air. Note that, in all three spectra, the $\nu$(N–N) region has been shown with an expanded absorbance scale. The photolysis times used to obtain the spectra were as follows: V, 5 min; Nb, 5 min; Ta, 4 min.

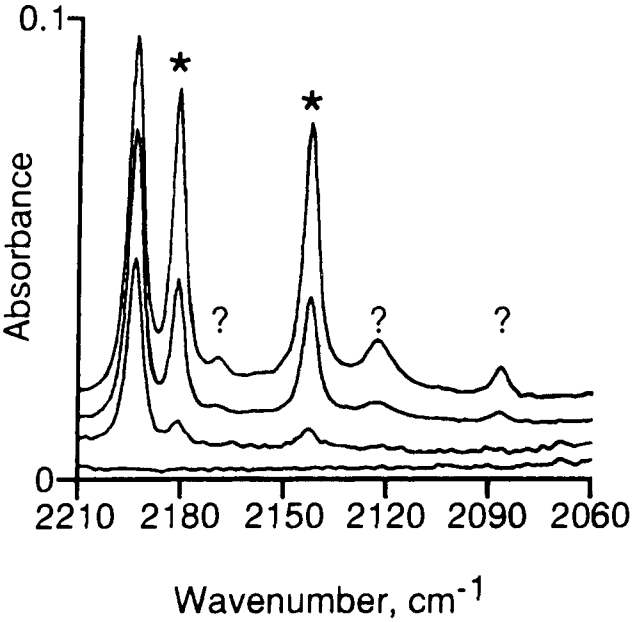


Figure 4. Series of FTIR spectra showing the growth of bands in the $\nu$(N–N) region during the UV photolysis of $CpNb(CO)_4$ in lXe doped with 120 psi of $N_2$ at −74 °C. The spectra, from the same experiment as that shown in Figure 3, were recorded before the start of photolysis and at subsequent intervals of 4, 4.5, and 5 min. The spectra have been offset vertically for easier visualization. Bands are identified as follows: unlabeled, $CpNb(CO)_3(N_2)$; *, $CpNb(CO)_2(N_2)_2$; ?, $CpNb(CO)(N_2)_3$ (tentative assignment).

constants can then be used to predict that the third $\nu$(C–O) fundamental should lie just to the low-wavenumber side (1911 $cm^{-1}$) of the relatively more intense a″ mode (1915 $cm^{-1}$), precisely in the position where a poorly resolved shoulder is observed (arrowed in Figure 2b). In addition, there is a single IR band at higher wavenumber due to the $\nu$(N–N) vibration of the coordinated $N_2$. The wavenumber of the natural abundance $^{14}N^{15}N$ satellite (Table I) confirms that the product contains only one $N_2$ group; the shift (35.7 $cm^{-1}$) observed between $\nu(^{14}N-^{14}N)$ and $\nu(^{14}N-^{15}N)$ is very close to that predicted (37.0 $cm^{-1}$) for an isolated harmonic diatomic $N_2$ oscillator while a $V-(N_2)_2$ moiety would be predicted to have a very much smaller isotopic shift because of vibrational coupling between the two $N_2$ groups. A very similar pattern of $\nu$(C–O) IR bands is seen in the TRIR spectrum obtained by flash photolysis of $CpV(CO)_4$ and $N_2$ in *n*-heptane at room temperature (Figure 2a). The only difference is that, even though the TRIR spectrum has lower resolution, the low-wavenumber shoulder fortuitously appears somewhat better resolved than that in lXe.

By contrast, the spectrum observed in solid $N_2$ matrices at 20 K contains a number of bands not observed in lXe (Figure 2c). Firstly, the "extra" $\nu$(N–N) band is most likely the result of the solid-state splittings frequently observed in matrices.[15] Such splitting of the $\nu$(N–N) band has also been reported by Rest and co-workers[14b] and is probably not significant. One of the $\nu$(C–O) bands, marked 3, has been assigned[14a] to a product with an $\eta^3$-$C_5H_5$ ring, which is either very short-lived or not formed at all in solution. More important to the characterization of $CpV(CO)_3(N_2)$ is the weaker $\nu$(C–O) band at 1875 $cm^{-1}$, arrowed. In previous matrix experiments,[14a] this band has been assigned to the third $\nu$(C–O) mode of $CpV(CO)_3(N_2)$. Our results are not consistent with this assignment for the following reasons: (i) The arrowed band does not have a constant intensity, relative to those of the other bands assigned to matrix-isolated $CpV(CO)_3(N_2)$; it is initially very weak, but in the later stages of photolysis, it is one of the strongest $\nu$(C–O) bands. (ii) The growth in intensity of this band appears to correlate with the growth of two additional $\nu$(N–N) bands (not illustrated), observed at 2204 and 2172 $cm^{-1}$ in pure $N_2$ matrices, and (iii) this band is not observed during photolysis of $CpV(CO)_4$ isolated in solid Ar doped with relatively small amounts of $N_2$. (iv) The band is not observed in our experiments in lXe (Figure 2b). Our suggestion, therefore, is that this $\nu$(C–O) band is due to a *disubstituted* species $(CpV(CO)_2(N_2)_2)$ formed by secondary photolysis, an assignment supported by the results of photolysis of $CpNb(CO)_3(N_2)$ in lXe solution.

**(b) Reaction of $CpNb(CO)_4$ and $CpTa(CO)_4$ with $N_2$.** Figure 3 compares the IR spectra obtained after UV photolysis of $CpM(CO)_4$ (M = V, Nb, and Ta) under similar conditions in lXe doped with $N_2$. In each spectrum, the unlabeled $\nu$(C–O) bands are due to residual $CpM(CO)_4$ and the bands colored black are assigned to the corresponding $CpM(CO)_3(N_2)$ complex. The wavenumbers of all of the bands are collected in Table I. A number of points are clear from the figure and table: (i) the bands of all three $CpM(CO)_4$ compounds are close in wavenumber; (ii) the $\nu$(C–O) bands of the three $CpM(CO)_3(N_2)$ products are also similar in frequency; (iii) although the $\nu$(N–N) band of $CpNb(CO)_3(N_2)$ is only slightly lower in wavenumber than that of $CpV(CO)_3(N_2)$, there is a much larger shift to low wavenumbers in the $\nu$(N–N) band of $CpTa(CO)_3(N_2)$; and (iv) there are three bands marked with asterisks, which are observed for Nb but for neither V nor Ta.

The $\nu$(N–N) spectra illustrated in Figure 4 show that these extra bands of Nb are not primary photolysis products but appear only in the later stages of the photolysis. These two bands and the corresponding $\nu$(C–O) band (not illustrated in Figure 4) are always observed with the same relative intensities and appear to be due to a single chemical species. Two $\nu$(N–N) bands, well separated in frequency, indicate the presence of two dinitrogen groups. We therefore assign these bands to the disubstituted species $(CpNb(CO)_2(N_2)_2)$ formed by secondary photolysis of $CpNb(CO)_3(N_2)$.

We favor the cis isomer (**5**) rather than the trans (**6**) on the basis of the relative intensities of the $\nu$(N–N) bands.[26] Although

(26) In bis-dinitrogen systems such **5** and **6**, the relative intensities of the symmetric and antisymmetric $\nu$(N–N) vibrations, $I_{sym}$ and $I_{antisym}$, are related by $I_{antisym}/I_{sym} = \tan^2(\theta/2)$, where $\theta$ is the angle between the two $N_2$ groups. Given that the two $\nu$(N–N) bands of $CpNb(CO)_2(N_2)_2$ are similar in intensity (Figures 3 and 4), we favor the cis structure **5** because the angle between the $N_2$ groups is smaller than that in **6**.

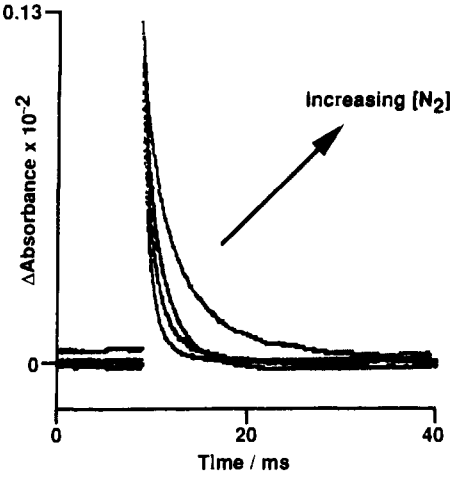


Figure 5. TRIR traces that show how increasing pressures of $N_2$ (from 0.5 to 2 atm) extend the lifetime of $CpV(CO)_3(N_2)$ generated by UV photolysis of $CpV(CO)_4$ in *n*-heptane at 25 °C; see also Table IIA. Signals were monitored at 1916 cm$^{-1}$.

such a species would be expected to have *two* $\nu$(C–O) bands, only one has been observed. However, a second band may well be

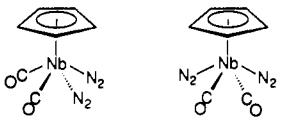


5 6

obscured by the $\nu$(C–O) bands of either $CpNb(CO)_4$ or $CpNb(CO)_3(N_2)$. The two bands labeled ? in Figures 3 and 4 are due to a thermally very labile species, possibly $CpNb(CO)(N_2)_3$, formed only in the final stages of the photolysis. The bands of $CpNb(CO)_2(N_2)_2$ are similar both in relative intensity and wavenumber to those tentatively assigned above to matrix-isolated $CpV(CO)_2(N_2)_2$. The fact that $CpV(CO)_2(N_2)_2$ is observed in solid $N_2$ but not in lXe is presumably the consequence of the very much higher effective concentration of $N_2$ in the matrix. Photochemical substitution of more than one CO group by $N_2$ in fluid solution is a relatively unusual reaction. Most previous examples have involved homoleptic metal carbonyl compounds or metal carbonyl nitrosyl complexes. Increasing ease of photosubstitution by $N_2$ in heavier transition metals is consistent with our observations[7,27a] in group 7, where UV photolysis of $CpRe(CO)_3$ in the presence of $N_2$ leads, eventually, to $CpRe(N_2)_3$, perhaps the best example of polysubstitution to be reported so far. Why $CpNb(CO)_4$ apparently undergoes polysubstitution more easily than $CpTa(CO)_4$ still remains unclear.[28]

$CpV(CO)_3(N_2)$ is thermally stable in lXe/$N_2$ at −78 °C for periods of several hours. Indeed, it can be generated thermally[16,22b] by reaction of $CpV(CO)_3(\eta^2\text{-}H_2)$ with $N_2$ in lXe at −78 °C. Unfortunately the concentrations of these species in lXe are too low for additional characterization by NMR.

$CpV(CO)_3(N_2)$ is not stable, however, in solution at room temperature, slowly reacting with CO to regenerate $CpV(CO)_4$ quantitatively. However, the TRIR kinetic traces illustrated in Figure 5 show that its lifetime can be extended by increasing the pressure of $N_2$ over the solution (Table IIA). Indeed quite modest pressures, e.g. 2 atm of $N_2$, give a lifetime of 30 ms (0.03 s). Such

(27) (a) Howdle, S. M.; Grebenik, P.; Perutz, R. N.; Poliakoff, M. *J. Chem. Soc., Chem. Commun.* **1989**, 1517. (b) Howdle, S. M.; Poliakoff, M. *J. Chem. Soc., Chem. Commun.* **1989**, 1099.

(28) We have observed that multiple substitution of CO groups in $CpV(CO)_4$ in lXe is possible. UV photolysis of $CpV(CO)_4$ in the presence of NO leads to formation of the known compound $CpV(CO)(NO)_2$, which is isoelectronic with $CpMn(CO)_3$. However, $CpV(CO)(NO)_2$ itself appears to be photochemically inert under the conditions of our experiments, and after venting the lXe/NO and refilling the cell with lXe/$H_2$ or lXe/$N_2$, we failed to observe any substitution of CO by $H_2$ or $N_2$.

Table II. Rate Constants for Pseudo-First-Order Thermal Decay in *n*-Heptane at 25 °C (All Rates Have an Error of Approximately ±10%)

| L | [L]/M | $k_{obs}$/s$^{-1}$ |
|---|---|---|
| | A. $CpV(CO)_3L$ | |
| $N_2$[a] | $4.8 \times 10^{-3}$ | $9.5 \times 10^2$ |
| | $9.5 \times 10^{-3}$ | $5.4 \times 10^2$ |
| | $1.5 \times 10^{-2}$ | $3.9 \times 10^2$ |
| | $1.9 \times 10^{-2}$ | $2.5 \times 10^2$ |
| $H_2$[b] | $2.3 \times 10^{-3}$ | $1.7 \times 10^3$ |
| | $9.0 \times 10^{-3}$ | $5.3 \times 10^2$ |
| $HSiEt_3$ | $1 \times 10^{-3}$ | $1.4 \times 10^3$ |
| | $1 \times 10^{-2}$ | $1.6 \times 10^2$ |
| | B. $V(CO)_5L$[c] | |
| $N_2$[a] | $1.9 \times 10^{-2}$ | $4.6 \times 10^3$ |
| $H_2$[b] | $9.0 \times 10^{-3}$ | $8.8 \times 10^3$ |

[a] A pressure of 1 atm of $N_2$ gives a concentration of dissolved $N_2$ equal to $9.5 \times 10^{-3}$ M. [b] A pressure of 1 atm of $H_2$ gives a concentration of dissolved $H_2$ equal to $4.5 \times 10^{-3}$ M. [c] The corresponding values[54] of $k_{obs}$, for $Cr(CO)_5(\eta^2\text{-}H_2)$ and 1.7 s$^{-1}$ for $Cr(CO)_5(N_2)$ in cyclohexane solution are 2.5 s$^{-1}$ at 1.3 atm. of $H_2$.

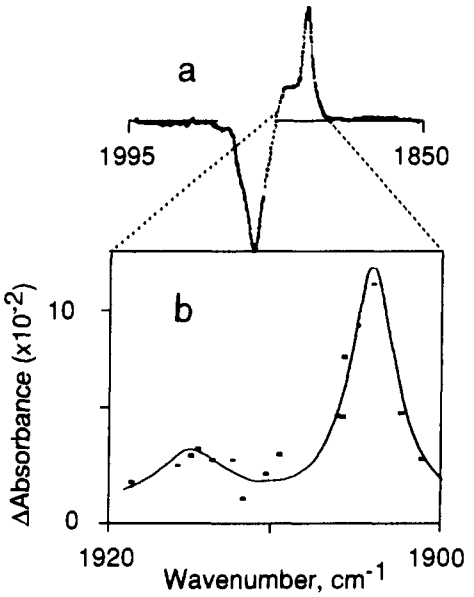


Figure 6. TRIR absorption spectra corresponding to a time 10 μs after the 308-nm flash photolysis of $CpV(CO)_4$ in *n*-heptane at room temperature in the presence of $H_2$. (a) Spectrum obtained with the line-tunable CO laser. The positive bands are due to $CpV(CO)_3(\eta^2\text{-}H_2)$ and the negative is due to $CpV(CO)_4$ destroyed by the flash. (b) High-resolution IR diode TRIR spectrum of the two bands of $CpV(CO)_3(\eta^2\text{-}H_2)$. The dots are experimental points. The solid line is *not* a computer fit but the superimposed FTIR spectrum of $CpV(CO)_3(\eta^2\text{-}H_2)$ recorded in lXe at −78 °C. Note that the line widths of the stronger peaks are the same in *n*-heptane and lXe.

behavior is consistent with reaction via a *dissociative* pathway (eq 3). The corresponding Nb and Ta dinitrogen compounds are significantly longer lived at room temperature, and their decay is too slow to be monitored accurately with our TRIR equipment.

$$CpV(CO)_3(N_2) \rightleftharpoons CpV(CO)_3 + N_2 \xrightarrow{+CO} CpV(CO)_4 \qquad (3)$$

**(c) Reactions with $H_2$.** Figure 6 shows TRIR spectra recorded during the reaction of $CpV(CO)_4$ with $H_2$ in *n*-heptane. The $\nu$(C–O) band of the product is similar to that of $CpV(CO)_3(N_2)$ (Figure 2a). Under the higher resolution of the IR diode laser, the S/N ratio is not as good but, nevertheless, the splitting of the bands can be seen to be very close to that observed for $CpV(CO)_3(\eta^2\text{-}H_2)$ in lXe solution (Figure 6b). Even at room temperature, there is no evidence for any bands attributable to a classical dihydride ($CpV(CO)_3H_2$). The rate of decomposition of $CpV(CO)_3(\eta^2\text{-}H_2)$ in *n*-heptane at room temperature shows a dependence on the pressure of $H_2$ (Table IIA), similar to that of

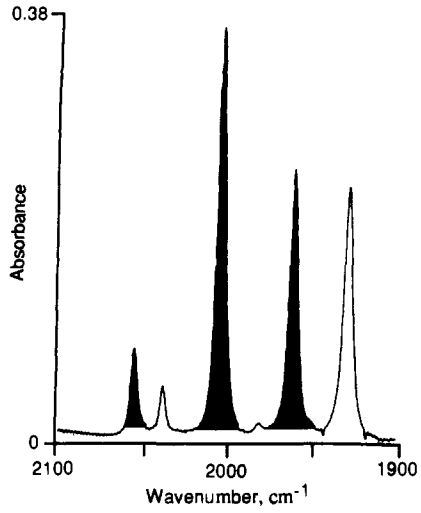


**Figure 7.** IR spectrum obtained by 15-min UV photolysis of $CpTa(CO)_4$ and $H_2$ in supercritical xenon at 20.2 °C (total pressure, 3260 psi; pressure of Xe, 1500 psi). The bands are assigned as follows: unlabeled, $CpTa(CO)_4$; colored, $CpTa(CO)_3H_2$, which decays over a period of ca. 30 min under these conditions, once the UV light has been switched off. For full experimental details of supercritical experiments, see ref 7. **Safety Note:** *Supercritical experiments involve high pressures and should not be undertaken without suitable precautions.*

$CpV(CO)_3(N_2)$ and $N_2$, cf. Figure 5. It is important to note, however, that this behavior does not in itself constitute a diagnostic test for a *nonclassical* dihydrogen complex because, as shown below, the lifetime of the dihydride $CpTa(CO)_3H_2$ can also be extended by high pressures of $H_2$.

Figure 7 shows the IR spectrum obtained after UV irradiation of $CpTa(CO)_4$ and a high pressure of $H_2$ in supercritical Xe (scXe) at room temperature.[29] One of the advantages of supercritical fluids as reaction media is that they are totally miscible with gaseous $H_2$. This means that a given pressure of $H_2$ will result in a significantly higher concentration of "dissolved" $H_2$ in a supercritical fluid than in a conventional solvent, an effect which we have used[7,27b] to stabilize species such as $CpMn(CO)_2(\eta^2\text{-}H_2)$ and which has since been exploited by others.[30] In the present case, the high concentration of $H_2$ sufficiently extends the lifetime of the dihydride $CpTa(CO)_3H_2$ for its spectra to be recorded by conventional FTIR. The $\nu$(C–O) bands of $CpTa(CO)_3H_2$, colored in Figure 7, are shifted to high wavenumber relative to those of $CpTa(CO)_4$, the consequence of oxidation of the metal center from Ta(I) to Ta(III).

Morris and co-workers have suggested that the wavenumber of the $\nu$(N–N) band of a $d^6$ $ML_x(N_2)$ complex provides an indication of whether the $ML_x$ fragment will form a classical or nonclassical complex when it reacts with $H_2$; a high wavenumber indicating poor $\pi$-backbonding and a high probability of forming a nonclassical dihydrogen complex.[31] The spectra in Figure 3 shows that such an argument also applies, at least qualitatively, to the $d^4$ $CpM(CO)_3$ fragments; $CpV(CO)_3(N_2)$ has its $\nu$(N–N) band at a wavenumber (2199.5 $cm^{-1}$) higher than that of $CpTa(CO)_3(N_2)$ (2164.5 $cm^{-1}$), consistent with $CpV(CO)_3$ forming a nonclassical dihydrogen complex and $CpTa(CO)_3$ a classical dihydride. The $\nu$(N–N) band of $CpNb(CO)_3(N_2)$ (2193.0 $cm^{-1}$) is only 6.5 $cm^{-1}$ lower than that of $CpV(CO)_3(N_2)$. Given that the energy difference between the classical and nonclassical Nb species is extremely small, the proximity of these $\nu$(N–N) bands suggests that the vanadium center may also be very close to the borderline between arrested and complete oxidative addition. Cp* rings are well-known to increase the electron density

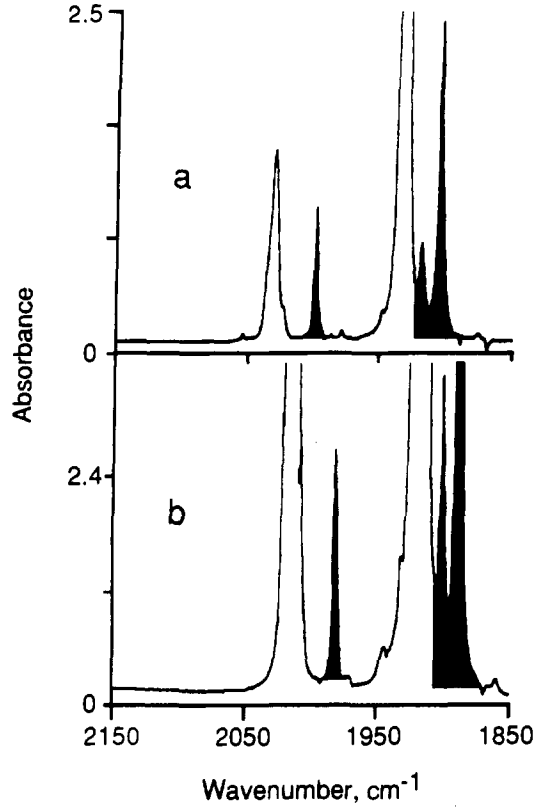


**Figure 8.** IR spectra in the $\nu$(C–O) region comparing the results of UV photolysis ($\lambda > 300$ nm) of (a) $CpV(CO)_4$ in lXe doped with 180 psi of $H_2$ and (b) $Cp^*V(CO)_4$ in lXe doped with 170 psi of $H_2$ at −70 °C. In each case, the bands are assigned as follows: unlabeled, starting material; colored, nonclassical dihydrogen reaction product. Photolysis times were (a) ca. 5 min and (b) ca. 10 min. Both spectra were run with relatively high concentrations of metal carbonyl (ca. $10^{-3}$ M) in an attempt to detect possible dihydride species. No bands attributable to dinuclear products were observed.

at a metal center compared to that of the analogous Cp complex. In most dihydrogen complexes, this increase has been too small to promote oxidative addition,[4] but in this case, energy differences may be smaller. Will $Cp^*V(CO)_3$ form classical or nonclassical species when reacting with $H_2$? Indeed, $Cp^*V(CO)_3(N_2)$ has its $\nu$(N–N) band at 2181 $cm^{-1}$ (see Table I), *lower* in wavenumber than that of $CpNb(CO)_3(N_2)$.

Figure 8 compares the $\nu$(C–O) regions of IR spectra obtained after the UV photolysis of (a) $CpV(CO)_4$ and (b) $Cp^*V(CO)_4$ in lXe doped with $H_2$. It is immediately clear, from both position and relative intensities of the colored bands, that the photoproducts are similar in the two reactions. There is a wavenumber shift in the bands of the Cp* photoproduct relative to those of $CpV(CO)_3(\eta^2\text{-}H_2)$, but the shift is comparable to that between the bands of the two starting compounds and is consistent with increased electron density on the metal center. Comparison of Figure 8b with the spectrum of $CpTa(CO)_3H_2$ (Figure 7) shows that, even with the rather large amount of $Cp^*V(CO)_3(\eta^2\text{-}H_2)$ present, there is no evidence for any bands which might be associated with even trace amounts of the dihydride $Cp^*V(CO)_3H_2$ in equilibrium with $Cp^*V(CO)_3(\eta^2\text{-}H_2)$. The presence of the $\eta^2\text{-}H_2$ ligand in the Cp* photoproduct is confirmed by the observation of a broad band in the region expected for the $\nu$(H–H) vibration (Figure 9a). TRIR experiments showed that both $Cp^*V(CO)_3(\eta^2\text{-}H_2)$ and $Cp^*V(CO)_3(N_2)$ are *longer* lived, by a factor of ca. 2, than their Cp analogs in *n*-heptane at room temperature.

Despite the ever growing number of nonclassical dihydrogen compounds,[4] IR data associated with $\nu$(H–H) vibrations remain sparse, because the bands are very weak and frequently masked by absorptions of solvent or other ligands. The three $\nu$(H–H) bands in Figure 9, represent a modest but rare opportunity to compare data from a set of closely related compounds. It is

(29) Details of our supercritical cells and experimental techniques can be found in refs 7 and 24 and references therein.

(30) Rathke, J. W.; Klingler, R. J.; Krause, T. R. *Organometallics* **1991**, *10*, 1350.

(31) Morris, R. H.; Earl, K. A.; Luck, R. L.; Lazarowych, N. J.; Sella, A. *Inorg. Chem.* **1987**, *26*, 2674.

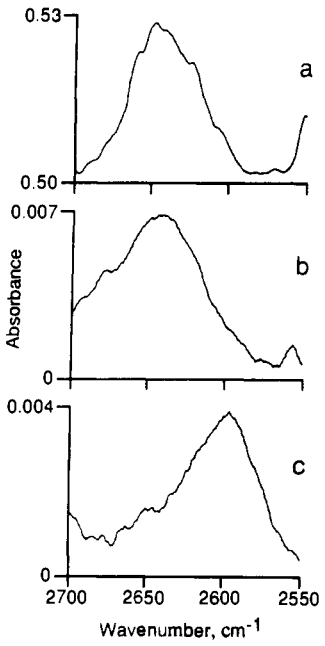


**Figure 9.** IR spectra in the $\nu$(H–H) region illustrating the absorptions of $\eta^2$-coordinated $H_2$ in (a) $Cp^*V(CO)_3(\eta^2\text{-}H_2)$, (b) $CpV(CO)_3(\eta^2\text{-}H_2)$, and (c) $CpNb(CO)_3(\eta^2\text{-}H_2)$. The bands were recorded in separate experiments. In each case, the dihydrogen complex was generated by UV photolysis of the appropriate tetracarbonyl compound in lXe solution under a pressure of $H_2$. These bands have been observed in several different experiments and the S/N ratio for each of these bands was greater than 15.

**Table III.** Wavenumbers ($cm^{-1}$) of $CpM(CO)_3(H_2$, HD, or $D_2)$ in Liquid Xenon at ca. 70 °C and in *n*-heptane at Room Temperature

| species | lXe[a] | *n*-heptane[b] | assignment |
|---|---|---|---|
| $CpV(CO)_3(\eta^2\text{-}H_2)$ | 2642 | | $\nu$(H–H) |
| | 1998.4 (1990.0)[c] | 1997 | a′ $\nu$(C–O) |
| | 1919.0 | 1917 1913.8[d] | a′ $\nu$(C–O) |
| | 1904.4 (1875.6) | 1908s 1905.3[d] | a″ $\nu$(C–O) |
| $CpV(CO)_3(\eta^2\text{-}HD)$ | 2377 | | $\nu$(H–D) |
| | 1998.0 | | a′ $\nu$(C–O) |
| | 1917.7 | | a′ $\nu$(C–O) |
| | 1903.6 | | a″ $\nu$(C–O) |
| $CpV(CO)_3(\eta^2\text{-}D_2)$[e] | 1998.3 | | a′ $\nu$(C–O) |
| | 1915.3 | | a′ $\nu$(C–O) |
| | 1903.5 | | a″ $\nu$(C–O) |
| $Cp^*V(CO)_3(\eta^2\text{-}H_2)$ | 2640 | | $\nu$(H–H) |
| | 1981.8 | 1986 | a′ $\nu$(C–O) |
| | 1900.9 | 1900[f] | a′ $\nu$(C–O) |
| | 1889.0 | 1891 | a″ $\nu$(C–O) |
| $CpNb(CO)_3(\eta^2\text{-}H_2)$ | 2600 | | $\nu$(H–H) |
| | 2000.7 (2000.7)[h] | g | a′ $\nu$(C–O) |
| | 1915.0 (1914.4)[h] | 1912 | a′ $\nu$(C–O) |
| | 1902.0 (1901.5)[h] | 1904 | a″ $\nu$(C–O) |
| $CpNb(CO)_3H_2$ | 2053.0 (2053.4)[i] | g | a′ $\nu$(C–O) |
| | 2006.0 (2005.9)[i] | g | a″ $\nu$(C–O) |
| | 1966.1 (1966.1)[i] | 1969 | a′ $\nu$(C–O) |
| $CpTa(CO)_3H_2$ | 2053.4 (2041.0)[c] | g | a′ $\nu$(C–O) |
| | 2001.8 (1978.2)[c] | g | a″ $\nu$(C–O) |
| | 1958.4 (1947.8)[c] | 1960 | a′ $\nu$(C–O) |

[a] FTIR, ±0.2 $cm^{-1}$. [b] CO laser TRIR, ±2 $cm^{-1}$. [c] Natural abundance $^{13}CO$ satellites. [d] Diode laser TRIR, ±0.5 $cm^{-1}$. [e] $\nu$(D–D) band not observed, presumably obscured by $\nu$(C–O) bands. [f] Shoulder. [g] Band outside tuning range of CO laser TRIR. [h] $\nu$(C–O) bands for $CpNb(CO)_3(\eta^2\text{-}D_2)$. [i] $\nu$(C–O) bands for $CpNb(CO)_3(D)_2$.

striking that the relative positions of the $\nu$(H–H) bands do not show any correlation with the relative wavenumber of the corresponding $\nu$(C–O) bands listed in Table III. Rather, they bear out our earlier contention,[32] based on a limited number of W compounds, that the position of the $\nu$(H–H) band is largely determined by the particular element to which the $\eta^2$-$H_2$ ligand is coordinated and is only marginally affected by other ligands attached to the same metal center.[34] As with other dihydrogen compounds, all three $\nu$(H–H) bands are very broad compared to the $\nu$(C–O) bands. Possible origins of this broadness have been discussed previously,[22a] and sadly, these spectra provide no further clues. Neither do the wavenumbers of the bands correlate with the thermal stability of the compounds; all three compounds are thermally labile, yet their $\nu$(H–H) bands are at *lower* wavenumbers than that of the prototypical dihydrogen complex $W(CO)_3(PCy_3)_2(\eta^2\text{-}H_2)$, which is thermally far more robust.[33]

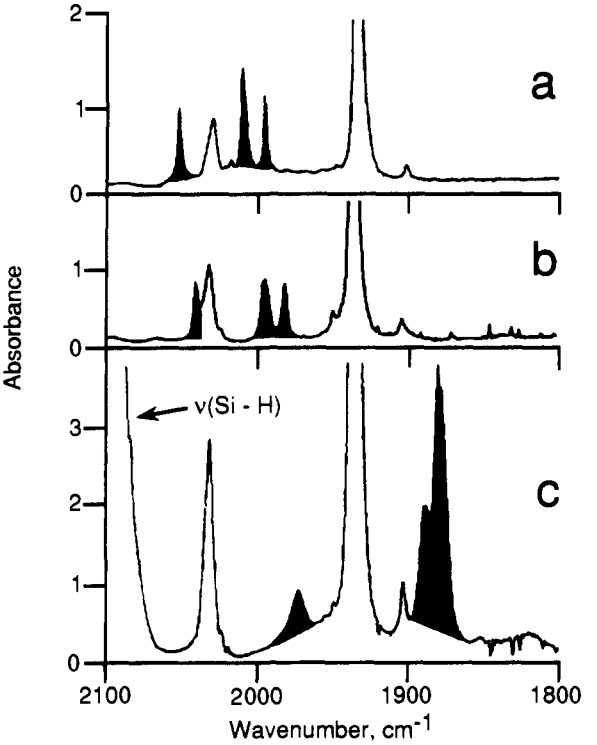


**Figure 10.** FTIR spectra showing the products of the photochemical reaction of $CpV(CO)_4$ in lXe solution with (a) $HSiCl_3$, (b) $HSiEtCl_2$, and (c) $HSiEt_3$ at −78 °C. In each spectrum, the bands of the photoproducts are colored and those of $CpV(CO)_4$ are unlabeled. The photolysis ($\lambda > 300$ nm) time was 15 min for all three silanes. Note the strong absorption in spectrum c due to the $\nu$(Si–H) vibration of the free $HSiEt_3$ in lXe solution. The corresponding $\nu$(Si–H) bands of $HSiEtCl_2$ and $HSiCl_3$ lie above 2100 $cm^{-1}$, outside the wavenumber range shown in this figure.

**(d) Reaction of $CpV(CO)_4$ with Silanes.** All of the experiments described so far indicate that addition of $H_2$ to $CpV(CO)_3$ or its $Cp^*$ analog does not lead to the formation of classical dihydrides. The nonclassical compound ($CpV(CO)_3(\eta^2\text{-}H_2)$, (**7**)) has five distinct ligands while the hypothetical $CpV(CO)_3H_2$ (**8**) would

(32) Jackson, S. A.; Hodges, P. M.; Jacke, J.; Poliakoff, M.; Turner, J. J.; Grevels, F.-W. (a) *J. Am. Chem. Soc.* **1990**, *112*, 1221; (b) **1990**, *112*, 1234.

(33) (a) Kubas, G. J.; Unkefer, C. J.; Swanson, B. I.; Fukushima, E. *J. Am. Chem. Soc.* **1986**, *108*, 7000. (b) Wasserman, H. J.; Kubas, G. J.; Ryan, R. R. *J. Am. Chem. Soc.* **1986**, *108*, 2294.

(34) Of course, $\nu$(H–H) is not the only vibration associated with the $\eta^2$-coordination of $H_2$, but it is, perhaps, the easiest to assign because it occurs in a characteristic region of the IR and with substantial isotopic shifts. We have endeavored to identify *lower* wavenumber bands due to the symmetric and antisymmetric M–($H_2$) vibrations of both the classical and nonclassical dihydride species. Our approach has been to generate both the $H_2$ and $D_2$ species by photolysis of the appropriate $CpM(CO)_4$ compound in lXe with $H_2$ or $D_2$ and to record the whole IR spectrum. It was hoped that lower wavenumber bands due to dihydrogen would be identifiable from definite isotopic shifts. Although the IR spectra did show differences not only between $H_2$ and $D_2$ but also between, V, Nb, and Ta, the identification of low-wavenumber bands was inconclusive, compared to the assignment of the $\nu$(H–H) and $\nu$(H–D) bands.[16,20] What the spectra did reveal were small but very reproducible shifts in $\nu$(C–O) bands between $H_2$, HD, and $D_2$, see Table III. These shifts in $\nu$(C–O) have allowed us to show that $CpV(CO)_4$ does not catalyze H/D exchange as was observed with $Cr(CO)_6$ in lXe solution doped with $H_2/D_2$ (Upmacis, R. K.; Poliakoff, M.; Turner, J. J. *J. Am. Chem. Soc.* **1986**, *108*, 3645).

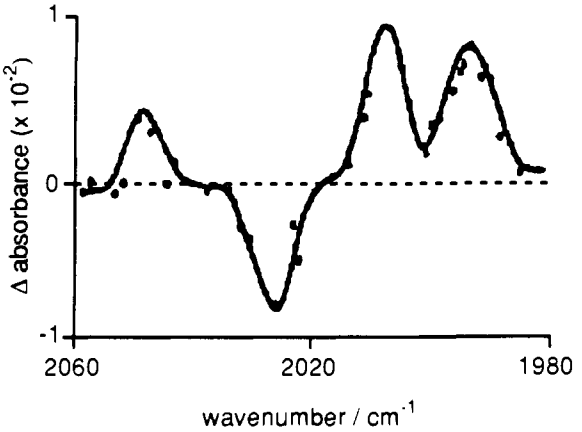


**Figure 11.** Diode laser TRIR spectrum showing the reaction of $CpV(CO)_4$ ($7 \times 10^{-4}$ M) and $HSiCl_3$ ($10^{-2}$ M) in *n*-heptane solution at room temperature. The spectrum corresponds to a time 10 μs after the UV flash. The positive bands are assigned to $CpV(CO)_3(H)SiCl_3$ (cf. Figure 10a), and the negative band is due to the $a_1$ ν(C–O) vibration of $CpV(CO)_4$.

have six ligands. Depending on how Cp is regarded, the V(III) center could be considered to be either seven or eight coordinate in $CpV(CO)_3H_2$. In such circumstances, it is reasonable to argue that steric crowding might favor formation of the nonclassical species. This argument can be tested by investigating the reaction of $CpV(CO)_4$ with silanes.

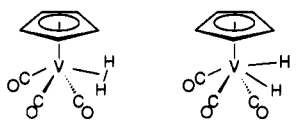

7 8

The photochemical reaction of $CpMn(CO)_3$ with silanes has been explored extensively.[3] Of particular relevance here are the reactions with $HSiEt_3$ and $HSiCl_3$, which lead to "arrested" and full oxidative addition of the H–$SiR_3$ bond, respectively. If steric factors were preventing full oxidative addition of $H_2$ to $CpV(CO)_3$, one would expect these factors to be even more important in the reaction with silanes. The reactions of $CpV(CO)_4$ with silanes have not been reported previously, so we have studied these reactions both in lXe[35] and in *n*-heptane.

Figure 10 shows spectra summarizing the results of our experiments in lXe; in each case, bands of the products were colored. Reaction of $CpV(CO)_4$ with $HSiCl_3$ yields almost identical spectra in lXe (Figure 10a) and in *n*-heptane (Figure 11). Similar results were obtained with $HSiCl_2Et$ (Figure 10b). In both cases, the ν(C–O) bands of the products are shifted to a wavenumber *higher* than those of the starting material ($CpV(CO)_4$), indicating an oxidation of the metal center. Although we could not detect any band assignable to a ν(V–H) vibration, presumably because it was too weak or obscured by the bands of the unreacted silane, the pattern of the ν(C–O) bands is very close to those of the $CpTa(CO)_3H_2$ classical dihydrides,[36] cf. Figure 7. Furthermore, reaction with $HSiCl_3$ caused an increase in the energy factored C–O stretching force constants and a decrease in the interaction constants relative to $CpV(CO)_4$ (Table IVB), changes which mirror those which occur between $CpTa(CO)_4$ and $CpTa(CO)_3H_2$. The

(35) The use of $HSiR_3$ compounds in lXe solution is not quite as straightforward as the use of $H_2$, because the silanes have strong ν(H–Si) IR bands just above the ν(C–O) region (see Figure 10c) and are not significantly volatile for easy removal at low temperature, a technique which we have previously exploited[32b] with $C_2H_4$.

(36) There are two possible isomers of $CpV(CO)_3(H)SiCl_3$ assuming a "five-legged" piano stool structure; the H and $SiCl_3$ can either be adjacent or separated by a CO group. In the case of $CpNb(CO)_3(H)_2$, we believed that the structure with adjacent H groups was the more likely given the facile equilibrium with $CpNb(CO)_3(\eta^2\text{-}H_2)$. Since the ν(C–O) spectrum of $CpV(CO)_3(H)SiCl_3$ is very similar to that of $CpNb(CO)_3(H)_2$, it is probable that the structures of the two compounds are the same.

Table IV. Wavenumbers and Energy Factored Force Constants

A. Wavenumbers ($cm^{-1}$) of $CpV(CO)_3(HSiEt_{3-x}Cl_x)$ Compounds in Liquid Xenon at ca. −70 °C and *n*-Heptane at Room Temperature

| species | lXe[a] | *n*-heptane | assignment |
|---|---|---|---|
| $CpV(CO)_3(\eta^2\text{-H–SiEt}_3)$ | 1971.8 | 1973[b] | a′ ν(C–O) |
| | 1887.0 | 1888[b,c] | a′ ν(C–O) |
| | 1877.1 [1852][d] | 1876[b] | a″ ν(C–O) |
| $CpV(CO)_3H(SiEtCl_2)$ | 2038.2 | | a′ ν(C–O) |
| | 1993.7/1992.1[e] | | a″ ν(C–O) |
| | 1979 [1966][d] | | a′ ν(C–O) |
| $CpV(CO)_3H(SiCl_3)$ | 2051.6 | 2049.6[f] | a′ ν(C–O) |
| | 2009.0 | 2008.5[f] | a″ ν(C–O) |
| | 1995.2 [1975][d] | 1994.8[f] | a′ ν(C–O) |

B. Energy Factored Force Constants (N $m^{-1}$) for $CpM(CO)_4$ and Various $CpM(CO)_3L$ Species (M = V and Ta) Calculated Using IR Data, Including $^{13}CO$ Satellites,[g] listed in Tables I, III, and IVA

| | $k_{CO}$ | $k_{cis}$ | $k_{trans}$ | |
|---|---|---|---|---|
| $CpV(CO)_4$ | 1541 | 38 | 45 | |
| $CpTa(CO)_4$ | 1542 | 44 | 45 | |
| | $k_1$[h] | $k_2$ | $k_{12}$ | $k_{22}$ |
| $CpV(CO)_3N_2$ | 1491 | 1529 | 40 | 47 |
| $CpV(CO)_3(\eta^2\text{-}H_2)$ | 1491 | 1537 | 40 | 50 |
| $CpV(CO)_3(\eta^2\text{-HSiEt}_3)$[i] | 1451 | 1506 | 40 | 52.5 |
| $CpV(CO)_3H(SiCl_3)$[i] | 1609 | 1665 | 7.5 | 35 |
| $CpTa(CO)_3H_2$ | 1554 | 1658 | 20 | 40 |
| $CpTa(CO)_3N_2$ | 1483 | 1506 | 45 | 49 |

[a] FTIR, ±0.2 $cm^{-1}$. [b] CO laser TRIR, ±2 $cm^{-1}$. [c] Shoulder. [d] Natural abundance $^{13}CO$ satellites. [e] Split band. [f] Diode laser TRIR, ±0.5 $cm^{-1}$. [g] With natural abundance $^{13}CO$ data, there are sufficient data to calculate all four force constants without making any assumptions. [h] $k_1$ refers to the unique CO group. [i] Calculated assuming $C_s$ symmetry.

silane products could not be generated in sufficient quantities for NMR characterization in more conventional solvents, but nevertheless, the IR spectra in Figures 10 and 11 are completely consistent both in frequency and relative intensity with full oxidative addition of $HSiCl_3$ to the V metal center, just in the same way as $HSiCl_3$ reacts with $CpMn(CO)_3$. Both $HSiCl_2Et$ and $HSiCl_3$ are sterically much more demanding than $H_2$. It is therefore clear that steric effects cannot be preventing oxidative addition of $H_2$ to the metal center.

By contrast, reaction of $CpV(CO)_4$ with $HSiEt_3$ in lXe leads to a spectrum (Figure 10c and Table IVA) quite different in the ν(C–O) region from that obtained with $HSiCl_3$. The wavenumbers of the ν(C–O) bands of the product are *lower* than those of $CpV(CO)_4$ itself, indicating the substitution of CO by a ligand which is primarily σ-donating in character. The relative intensities of the ν(C–O) bands are similar to those of $CpV(CO)_3(\eta^2\text{-}H_2)$ (Figure 8a). The data in Table IVA show that the same reaction can be observed by TRIR in *n*-heptane solution at room temperature. Under these conditions, the lifetime of the product is extended by increasing the concentrations of $HSiEt_3$ in solution, an effect similar to that previously observed for $CpV(CO)_3L$ (L = $N_2$ or $\eta^2\text{-}H_2$; Table IIA and Figure 5). In addition, reaction with $HSiEt_3$ causes changes in the energy factored force constants (Table IVB) very similar to those observed for reaction with $H_2$ and $N_2$. These spectroscopic and kinetic data are consistent with *arrested* oxidative addition of $HSiEt_3$ to form $CpV(CO)_3(\eta^2\text{-H–SiEt}_3)$. Although the evidence is clearly still circumstantial, such a compound represents a significant extension to the known examples of arrested oxidative addition of H–$SiR_3$, since it involves a new metal center and a new d electron configuration. It is unlikely that $CpV(CO)_3(\eta^2\text{-H–SiEt}_3)$ itself could be isolated, but it is quite probable that, with suitable choice of substituents, a stable complex of this type could be synthesized.

Our results, both in lXe and at room temperature, suggest that steric factors are not the determining factor in preventing full oxidative addition of $H_2$ to the $CpV(CO)_3$ moiety. Electronic factors appear to be more important. It is striking that, in all of the reactions described above, the behavior of $CpV(CO)_4$ has been similar to that of $CpMn(CO)_3$, despite differences in both the

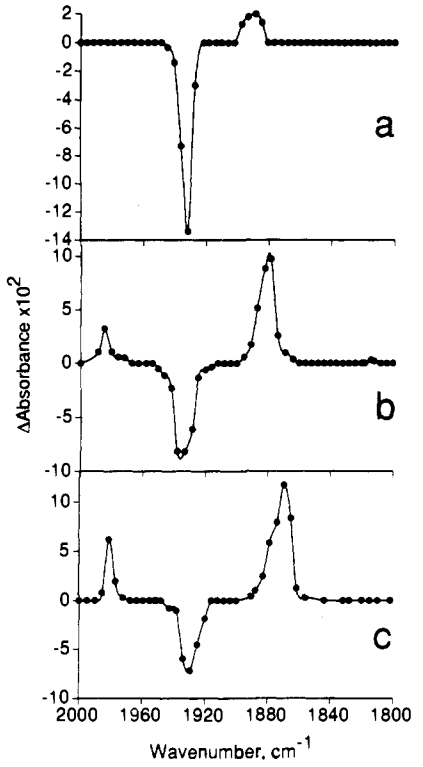


Figure 12. TRIR spectra (CO laser) obtained by 308-nm photolysis of $CpM(CO)_4$ in *n*-heptane under 2 atm of CO, showing the formation of $CpM(CO)_3$ intermediates for (a) V, 125 ns after the UV flash, and (b) Nb and (c) Ta, both 2 μs after the UV flash. In each case the positive bands are due to $CpM(CO)_3$ and the negative to $CpM(CO)_4$.

electron count and the geometry at the metal center. Nevertheless, all of the $CpV(CO)_3L$ species have been consistently more labile than the corresponding $CpMn(CO)_2L$ compounds. This difference is even more marked in the kinetics of the reaction intermediates.

**2. Reaction Kinetics and Identification of Intermediates. (a) Identification of $CpM(CO)_3$.** All of the reactions described in the first part of this paper have involved the photochemical substitution of one, or occasionally two, CO groups in $CpM(CO)_4$ and substitution by $N_2$, $H_2$, or $HSiR_3$, sometimes with oxidative addition, but more frequently, without. Our aim now is to establish whether these reactions share a common mechanism and to identify at least the more important intermediates. These has been relatively little previous work in this area. Thermal substitution reactions of $CpM(CO)_4$ compounds have been studied for V,[37a,b] Nb, and Ta,[37c] and both dissociative and associative pathways appear to be significant. Rest and co-workers[14] have studied the photolysis of $CpV(CO)_4$ and related V compounds isolated in inert matrices and have reported ν(C–O) IR data for both $CpV(CO)_3$ and a species identified as $(\eta^3\text{-}C_5H_5)V(CO)_4$, formed by "slippage" of the $\eta^5$-Cp ring. Analogous reactions of $CpMn(CO)_3$ have been shown to proceed largely via the formally unsaturated species $CpMn(CO)_2$···s, where s represents a solvent molecule acting as an easily exchanged token ligand occupying the otherwise vacant coordination site.[8,9] Thus, our experiments have involved extensive TRIR experiments on $CpM(CO)_4$ (M = V, Nb, and Ta) in *n*-heptane at room temperature in the presence of Ar, CO, $N_2$, $H_2$, or $HSiR_3$ with some supporting matrix isolation experiments, where necessary.

Figure 12 shows short-time-scale CO laser TRIR spectra for 308-nm photolysis of the $CpM(CO)_4$ complexes of V, Nb, and Ta in *n*-heptane. The IR bands in these spectra can be assigned to $CpM(CO)_3$ species for the following reasons; (i) for each metal, the same absorptions are observed even in the absence of potential ligands (e.g. CO, $N_2$, $H_2$, etc.) in the solution; (ii) the spectra are in reasonable agreement with the available matrix data for $CpM(CO)_3$, see Table V; and (iii) in each case, the bands decay faster in the presence of added CO and their rates of decay are *exactly* matched by the rate of regeneration of $CpM(CO)_4$, as expected from eq 4, see Figure 13.

$$CpM(CO)_3 + CO \rightarrow CpM(CO)_4 \qquad (4)$$

The assignment is further supported not only by the similarity of the spectra of $CpNb(CO)_3$ and $CpTa(CO)_3$ to each other (Figure 12b and c) but also by their obvious resemblance to the spectra of the various $CpM(CO)_3L$ species described above. $CpV(CO)_3$ is nearly 2 orders of magnitude more reactive than the corresponding Nb and Ta species (see Figure 13) and can only be detected by TRIR measurements made on a much shorter time scale. Faster measurements are noisier, but nevertheless, the TRIR spectrum for vanadium (Figure 12a) shows a broad ν(C–O) band close in wavenumber to the most intense of the bands assigned[14a] by Hitam and to that of matrix-isolated $CpV(CO)_3$.[38]

**(b) Reaction Kinetics of $CpM(CO)_3$.** In all of the TRIR experiments, the fraction of $CpM(CO)_4$ destroyed by the UV flash is relatively small, usually 5–10%. In these circumstances, potential reactants are usually present in solution at concentrations

Table V. Wavenumbers ($cm^{-1}$) of $CpM(CO)_3$ Species in *n*-Heptane at Room Temperature and in Cryogenic Matrices

| species | *n*-heptane[a] | matrix: Ar | matrix: $CH_4$ | tentative assignment[d] |
|---|---|---|---|---|
| $CpV(CO)_3$ | | 1964.4[b] | 1953.5[c] | a′ ν(C–O) |
| | 1895 | 1901.8[b] | 1887.0[c] | a″ ν(C–O) |
| | | 1866.6[b] | 1858.9[c] | a′ ν(C–O) |
| | | | 1856.2[c] | |
| $Cp^*V(CO)_3$ | | | 1979[e] | a′ ν(C–O) |
| | 1878 | 1880[f] | | a″ ν(C–O) |
| $CpNb(CO)_3$ | 1986 | | | a′ ν(C–O) |
| | 1885 (broad) | | | a′ + a″ ν(C–O) |
| $CpTa(CO)_3$ | 1980 | 1987[h] | | a′ ν(C–O) |
| | 1880[g] | 1880[h] | | a′ ν(C–O) |
| | 1873 | 1874[h] | | a″ ν(C–O) |

[a] CO laser TRIR, ±2 $cm^{-1}$. [b] Ar matrix.[14a] [c] $CH_4$ matrix.[14a] [d] Assignment based on a $C_s$ geometry for $CpM(CO)_3$. [e] $CH_4$ matrix.[14b] [f] Ar matrix,[14b] 20 K. [g] Shoulder, barely resolved, see Figure 13c. [h] Ar matrix, this work.

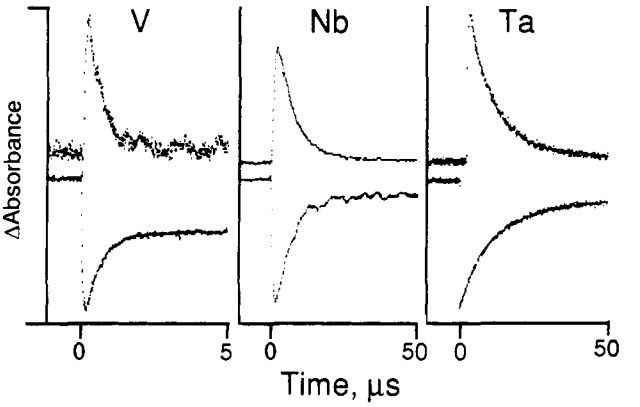


Figure 13. TRIR kinetic traces showing the recombination of $CpM(CO)_3$ with CO to regenerate $CpM(CO)_4$ (M = V, Nb, and Ta). All traces were recorded in *n*-heptane under a pressure of 2 atm of CO. IR monitoring wavenumbers were as follows: $CpV(CO)_3$, 1895 $cm^{-1}$, and $CpV(CO)_4$, 1932 $cm^{-1}$; $CpNb(CO)_3$, 1885 $cm^{-1}$, and $CpNb(CO)_4$, 1932 $cm^{-1}$; $CpTa(CO)_3$, 1873 $cm^{-1}$, and $CpTa(CO)_4$, 1923 $cm^{-1}$. Note the much faster time base of the measurement for vanadium. The absorbance scales of the different traces have been normalized.

(37) (a) Faber, G.; Angelici, R. J. *Inorg. Chem.* **1970**, *9*, 1586. Value of $\Delta H^*$ corrected: *Inorg. Chem.* **1984**, *23*, 4781. (b) Kowaleski, R. M.; Kipp, D. O.; Stauffer, K. J.; Swepston, P. N.; Basolo, F. *Inorg. Chem.* **1985**, *24*, 3750. (c) Freeman, J. W.; Basolo, F. *Organometallics* **1991**, *10*, 256.

(38) The assignment[14a] of the spectrum of matrix-isolated $CpV(CO)_3$ suggests that the position of the lower frequency a′ band is significantly lower in wavenumber than that in $CpNb(CO)_3$ and $CpTa(CO)_3$. We did not observe any transient TRIR signals at this wavenumber, but given the relatively poor S/N, we cannot eliminate the possibility of a weak absorption in this region.

Table VI. Kinetic Data for the Reaction of $CpM(CO)_3$ with Different Ligands, L, in *n*-heptane at 25 °C[a]

| $CpM(CO)_4/L$[b] | [L]/M | $k_{obs}/s^{-1}$ | $k_2/M^{-1}\ s^{-1}$ |
|---|---|---|---|
| $CpV(CO)_4/Ar$ | | $5.4 \times 10^5$ | |
| $CpV(CO)_4/N_2$ | $1.9 \times 10^{-2}$ | $2.9\ (2.8) \times 10^6$ | $1.5\ (1.5) \times 10^8$ |
| $CpV(CO)_4/H_2$ | $9.0 \times 10^{-3}$ | $2.0\ (1.9) \times 10^6$ | $2.2\ (2.1) \times 10^8$ |
| $CpV(CO)_4/CO$ | $2.4 \times 10^{-2}$ | $3.2 \times 10^6$ | $1.3 \times 10^8$ |
| $CpV(CO)_4/HSiEt_3$ | $1.0 \times 10^{-2}$ | $2.0\ (1.8) \times 10^6$ | $2.0\ (1.8) \times 10^8$ |
| $Cp^*V(CO)_4/Ar$ | | $4.7 \times 10^5$ | |
| $Cp^*V(CO)_4/N_2$ | $1.9 \times 10^{-2}$ | $7.2\ (6.9) \times 10^6$ | $3.6\ (3.4) \times 10^8$ |
| $Cp^*V(CO)_4/H_2$ | $9.0 \times 10^{-3}$ | $5.4\ (5.2) \times 10^6$ | $6.0\ (5.7) \times 10^8$ |
| $CpNb(CO)_4/CO$ | $2.4 \times 10^{-2}$ | $1.7 \times 10^5$ | $7.0 \times 10^6$ |
| $CpNb(CO)_4/N_2$ | $1.9 \times 10^{-2}$ | $9.3\ (9.1) \times 10^4$ | $4.9\ (4.8) \times 10^6$ |
| $CpNb(CO)_4/H_2$[c] | $9.0 \times 10^{-3}$ | $6.7\ (6.7) \times 10^4$ | $7.4\ (7.4) \times 10^6$ |
| $CpNb(CO)_4/H_2$[d] | $9.0 \times 10^{-3}$ | $6.7\ (7.0) \times 10^4$ | $7.4\ (7.8) \times 10^6$ |
| $CpTa(CO)_4/Ar$ | | $5.9 \times 10^3$ | |
| $CpTa(CO)_4/CO$ | $2.4 \times 10^{-2}$ | $1.2 \times 10^5$ | $5.0 \times 10^6$ |
| $CpTa(CO)_4/N_2$ | $1.9 \times 10^{-2}$ | $5.5\ (5.4) \times 10^4$ | $2.9\ (2.8) \times 10^6$ |
| $CpTa(CO)_4/H_2$ | $9.0 \times 10^{-3}$ | $3.0\ (4.5) \times 10^4$ | $3.3\ (5.0) \times 10^6$ |

[a] Rate constants are for the disappearance of $CpM(CO)_3$ and those in parentheses are for the corresponding appearance of $CpM(CO)_3L$. [b] For concentrations of $CpM(CO)_4$, see Experimental section. [c] Rate for formation of $CpNb(CO)_3(\eta^2\text{-}H_2)$. [d] Rate for formation of the dihydride $CpNb(CO)_3H_2$.

which are high compared to those of $CpM(CO)_3$. Surprisingly, even in the absence of added ligands (i.e. under 2-atm pressure of Ar), the decay of $CpM(CO)_3$ follows pseudo-first-order kinetics (Table VI), most probably through reaction with excess starting material to form dimeric species, as was found for the $CpMn(CO)_3$ system.[8a] Under an Ar atmosphere, the TRIR spectrum corresponding to 10 μs after the UV flash photolysis of $CpV(CO)_4$ shows a very weak and almost continuous IR absorption across the region 2000–1850 $cm^{-1}$. These is, however, no evidence for the formation of the known dinuclear compound[39] $Cp_2V_2(CO)_5$ as a significant product. In the presence of added ligands (e.g. CO, $H_2$, $N_2$, etc.), these weak bands are largely suppressed and the TRIR spectra show the expected bands of the appropriate $CpV(CO)_3L$ species (e.g. Figures 2a and 6).[40] The data in Table VI confirm that, in every case, the rate of formation of $CpV(CO)_3L$ matches very closely the decay of $CpV(CO)_3$, as expected from eq 5.

$$CpV(CO)_3 + L \xrightarrow{k_{obs}} CpV(CO)_3L \qquad (5)$$

Calculating the bimolecular rate constants for the reactions of $CpV(CO)_3$ from these values of $k_{obs}$ presents problems because, even under 2 atm of CO, the regeneration of $CpV(CO)_4$ is not complete (see Figure 13). In previous studies,[32] we have successfully used the relationship $k_{obs} = k_2[L] + k_{Ar}$, where $k_{Ar}$ is the first-order constant for decay in the *absence* of added ligands. We have accumulated extensive data for $CpV(CO)_3$ by varying the concentration of added ligands. The relatively large value of $k_{Ar}$ means that the errors are large, but the data appear to fit this relationship, which has been used to calculate the values of $k_2$ in Table VI. Rate constants for the corresponding reactions of $CpNb(CO)_3$ and $CpTa(CO)_3$ are also collected in Table VI. The values of both $k_{obs}$ and $k_2$ for $CpV(CO)_3$ are substantially larger than those for Nb and Ta, which are similar to each other but still significantly larger than the corresponding values[8] for $CpMn(CO)_2$. It is significant that, for both Nb and Ta, similar rate constants are found for reaction with $H_2$, which leads to oxidative addition, and with $N_2$, which does not.

Figure 14 shows TRIR traces for the reaction of $H_2$ with $CpV(CO)_3$ and $Cp^*V(CO)_3$ to form the corresponding dihydrogen compounds. Both tricarbonyl intermediates are very short-lived, and the greater reactivity of the Cp* species toward $H_2$ exactly mirrors the behavior[8b] of $Cp^*Mn(CO)_2$ relative to $CpMn(CO)_2$,

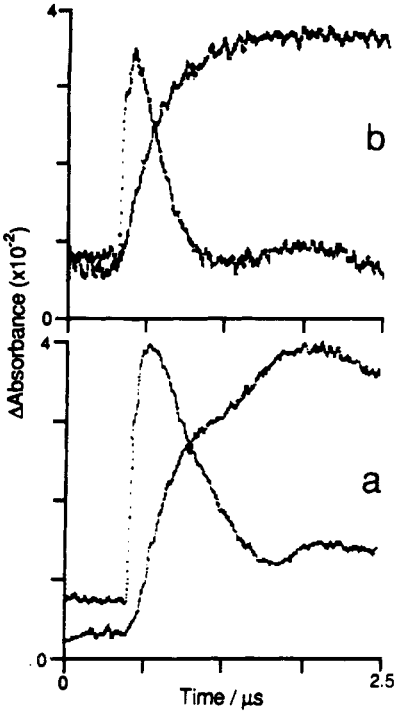


Figure 14. TRIR kinetic traces recorded during the UV flash photolysis of $(C_5R_5)V(CO)_4$ in *n*-heptane at room temperature under 2-atm pressure of $H_2$: (a) R = H; (b) R = Me. The traces show the transient generation of $(C_5R_5)V(CO)_3$ and formation of $(C_5R_5)V(CO)_3(\eta^2\text{-}H_2)$. IR monitoring wavenumbers were (a) 1895 and 1908 $cm^{-1}$ and (b) 1877 and 1899 $cm^{-1}$. Note that the undulations in the $CpV(CO)_3$ trace in part a are due to shock waves generated by the UV flash.

but on a much shorter time scale. Indeed $Cp^*V(CO)_3$ is probably the most reactive intermediate formed by loss of CO from a carbonyl compound to have been observed so far in solution by TRIR.

**(c) Interaction of $CpM(CO)_3$ with *n*-Heptane: Photoacoustic Calorimetry.** It is becoming apparent that most, if not all, 16-electron species formed by photoejection of CO from a metal carbonyl compound are solvated even in hydrocarbon solvents.[41] Although the presence of these solvating hydrocarbons has never been observed directly, the accumulated volume of circumstantial evidence is huge and convincing. We would therefore expect that the $CpM(CO)_3$ (M = V, Nb, and Ta) intermediates would be similarly solvated. Photoacoustic experiments with $CpV(CO)_4$ provide evidence consistent with such solvation.[19]

Photoacoustic calorimetry (PAC) has been quite extensively used to study energetics of organometallic reactions.[42] In essence, PAC involves the use of a photochemical reaction cell fitted with a sensitive microphone which monitors the shock wave generated during pulsed laser irradiation of the solution. PAC measurements involve two stages: first, the use of a non-photoactive compound, in this case ferrocene, to calibrate the system and, then, the measurement on the photochemical reaction in question. The

(39) Lewis, L.; Caulton, K. G. *Inorg. Chem.* **1980**, *19*, 1840.

(40) Reaction with excess $CpV(CO)_4$ is not observed in lXe experiments because the concentration of $CpV(CO)_4$ is at least 1 order of magnitude lower than that in *n*-heptane and the concentration of dissolved gas (e.g. $N_2$) is more than an order of magnitude higher, not only because of the higher pressure of gas over the solution but also because of the lower temperature.

(41) For an up-to-date review on $Cr(CO)_5$ and its interactions, see: Turner, J. J. In *Photoprocesses in Transition Metal Complexes, Biosystems and Other Molecules*; Kochanski, E., Ed.; NATO ASI Series; Springer: New York, in press. *ASI Series C Mathematical & Physical Sciences*; Kluwer Academic Publishers: Dordrecht, 1992; Vol. 376, p 125.

(42) For a selection of applications of PAC to organometallic compounds, see: (a) Bernstein, M.; Simon, J. D.; Peters, K. S. *Chem. Phys. Lett.* **1983**, *100*, 241. (b) Rudzki, J. E.; Goodman, J. L.; Peters, K. S. *J. Am. Chem. Soc.* **1985**, *107*, 7849. (c) Yang, G. K.; Peters, K. S.; Vaida, V. *Chem. Phys. Lett.* **1986**, *125*, 566; *Polyhedron* **1988**, *7*, 1619. (d) Nolan, S. P.; Hoff, C. D.; Stoutland, P. O.; Newman, L. J.; Buchanan, J. M.; Bergman, R. O.; Yang, G. K.; Peters, K. S.; *J. Am. Chem. Soc.* **1987**, *109*, 3143. (e) Burkey, T. J. *Polyhedron* **1989**, *8*, 2681. (f) Morse, J. M., Jr.; Parker, G. H.; Burkey, T. J. *Organometallics* **1989**, *8*, 2471. Burkey, T. J. *J. Am. Chem. Soc.* **1990**, *112*, 8329. (g) Klassen, J. K.; Selke, M.; Sorensen, A. A.; Yang, G. K. *J. Am. Chem. Soc.* **1990**, *112*, 1267. (h) Nayak, S. K.; Burkey, T. J. *Abstracts of Papers*, 204th National Meeting of the American Chemical Society, Washington, DC, August 1992; Inorganic Division Abstract 48.

**Table VII.** Enthalpy Changes (kJ mol$^{-1}$) Measured by Photoacoustic Calorimetry[a]

| reaction | | | $\Delta H^{b,c}$ |
|---|---|---|---|
| $CpV(CO)_4$ + *n*-heptane | → $CpV(CO)_3$(*n*-heptane) | + CO | 107 ± 13 |
| $CpV(CO)_4 + H_2$ | → $CpV(CO)_3(\eta^2\text{-}H_2)$ | + CO | 56 ± 5 |
| $CpV(CO)_4 + N_2$ | → $CpV(CO)_3(N_2)$ | + CO | 27 ± 4 |
| $CpV(CO)_4$ + CO | → $CpV(CO)_4$ | + CO | 0 ± 1 |

[a] Taken from ref 19. [b] Assuming quantum yield of 0.8 for all reactions. [c] All errors are maximum deviation of measured values.

enthalpy of the reaction can then be derived directly from the expression eq 6, where $E_{ref}$ and $E_{phol}$ are the energy released in

$$\Delta H^\circ = (E_{ref} - E_{phol})/\Phi \quad (6)$$

the reference and photochemical measurements, respectively, and $\Phi$ is the quantum yield, the value of which is clearly a key feature of the experiment. In its simplest form, the method can only be used with reactions that are faster than 1 μs. Thus, this method has been particularly successful for evaluating the enthalpy associated with reactions of the type shown in eq 7. An estimate

$$L_nM(CO)_x + \text{solvent} \xrightarrow{UV} L_nM(CO)_{x-1}(\text{solvent}) + CO \quad (7)$$

of the strength of the M···solvent interaction can then be obtained from the difference between the enthalpy change for such a reaction and the enthalpy of activation for thermal substitution reactions of $L_nM(CO)_x$ or related compounds. This approach has now been successfully applied to $CpMn(CO)_2$···(heptane)[9] and to $M(CO)_5$ intermediates of group 6 metals,[42c] where the interaction energies are consistent with those measured by other techniques in the gas phase.[43]

We have carried out a limited number of PAC experiments with $CpV(CO)_4$, with the aim of investigating the interaction between the vanadium center and weakly coordinating ligands, including *n*-heptane. $CpV(CO)_4$ is particularly suited to such studies because the high reactivity of $CpV(CO)_3$ permits the study of reactions with $H_2$ and $N_2$ without complicated computer deconvolution of the PAC signals. The major innovation of these experiments was to combine PAC and TRIR measurements by fitting the PAC cell with IR transparent windows. This has allowed us to compare the quantum yields for reaction with $H_2$ and $N_2$ with the previously reported value[12a] for reaction with $PPh_3$. The procedure involved tuning the CO laser of the TRIR apparatus to 1932 cm$^{-1}$, coincident with the stronger $\nu$(C–O) band of $CpV(CO)_4$. Three measurements were then made; each measurement involved a solution with a standard concentration of $CpV(CO)_4$, which was irradiated with a single pulse from the UV laser (308 nm) in the presence of the appropriate ligand (i.e. $H_2$, $N_2$, or $PPh_3$), and the amount of $CpV(CO)_4$ destroyed by the UV pulse was measured via the TRIR signal. The use of only one laser pulse effectively eliminates possible errors from secondary photolysis. Assuming that the quantum yield for reaction with $PPh_3$ is 0.8 at this wavelength,[12a] our TRIR measurements[44] gave quantum yields of 0.83 (±0.07, maximum error) for reaction with $H_2$ and 0.78 (±0.06) for reaction with $N_2$. Table VII summarizes the enthalpy changes derived from our PAC measurements on $CpV(CO)_4$, using the same value (0.8) for the quantum yields of all of the reactions. A number of points are important in the context of the present paper: (i) A zero enthalpy change was observed when $CpV(CO)_4$ was photolysed under CO, indicating that the photolysis is *completely* reversible within 1 μs under these conditions.[45] (ii) The measurements indicate that the V-($\eta^2$-$H_2$) bond is significantly weaker (29 ± 9 kJ mol$^{-1}$) than the V–$N_2$ bond. This is consistent with the thermal displacement of $\eta^2$-$H_2$ by $N_2$ described above and in broad agreement with thermochemical measurements on less reactive dihydrogen compounds.[46] (iii) The bond dissociation energy for the V-($\eta^2$-$H_2$) bond (91 ± 20 kJ mol$^{-1}$) is, surprisingly, somewhat larger than the value (71 kJ mol$^{-1}$) very recently derived for the $(CO)_5$Cr-($\eta^2$-$H_2$) bond from PAC measurements.[42h] It is also comparable to the enthalpy of heterogeneous adsorption of $H_2$ onto the surface of many first-row transition metals. (iv) The enthalpy for the reaction $CpV(CO)_4$ + *n*-heptane → $CpV(CO)_3$(*n*-heptane) (107 ± 13 kJ mol$^{-1}$) is significantly less than the activation enthalpy[37a] (148 ± 2 kJ mol$^{-1}$) for thermal reactions of $CpV(CO)_4$, indicating that there is indeed interaction between $CpV(CO)_3$ and the solvent. Although these data suggest that the interaction is of comparable strength (41 ± 15 kJ mol$^{-1}$) to that estimated for the $CpMn(CO)_2$···(*n*-heptane) interaction,[9] the cumulative errors in this value are quite large. However, given that the reactivity of $CpV(CO)_3$ is much greater than the reactivity of $CpMn(CO)_2$, the true strength of the $CpV(CO)_3$···(*n*-heptane) interaction is almost certainly less than that of the $CpMn(CO)_2$···(*n*-heptane) interaction.

Although PAC measurements have not as yet been carried out on $CpNb(CO)_4$ or $CpTa(CO)_4$, it is reasonable to suppose that the $CpM(CO)_3$ intermediates in these systems will also interact with the solvent. It is also probable the M···(*n*-heptane) interactions would be stronger than those for V given that all of the other $CpV(CO)_3L$ species described above have been more labile than their Nb and Ta congeners.

**3. Comparison with $V(CO)_6$: Detection of $V(CO)_5$, $V(CO)_5(N_2)$, and $V(CO)_5(\eta^2\text{-}H_2)$.** Unlike the group 7 metals, vanadium forms a stable mononuclear binary carbonyl compound ($V(CO)_6$). With its $d^5$ electron configuration, $V(CO)_6$ offers an interesting reference point for comparing the behavior not only of $d^4$ $CpV(CO)_4$ but also of $d^6$ $CpMn(CO)_3$ and $Cr(CO)_6$. Unlike $Cr(CO)_6$, $V(CO)_6$ undergoes extremely facile thermal reactions[47] many orders of magnitude faster than those of $Cr(CO)_6$. Probably for this reason, the photochemical reactions of $V(CO)_6$ have not been studied extensively. TRIR experiments on $V(CO)_6$ in the gas phase[48] have provided evidence for formation of $V(CO)_4$ and $V(CO)_5$ as well as of a dinuclear species, probably $V_2(CO)_{10}$, formed by reaction of $V(CO)_4$ with excess $V(CO)_6$. There have been a number of matrix isolation studies involving both photolysis[49a] of $V(CO)_6$ and cocondensation[49b] of V atoms with CO. However, the results are much less precise than those for $Cr(CO)_6$, because the Jahn–Teller instability of $V(CO)_6$ gives rise to substantial broadening of the $\nu$(C–O) bands.[49b] This broadening prevents $^{13}CO$ isotopic substitution from being exploited fully to determine the geometry of the various $V(CO)_x$ species. Given this lack of photochemical data, we have carried out lXe and TRIR experiments[50] with $V(CO)_6$ to identify the products of its reaction with $N_2$ and $H_2$. The reaction with $H_2$ has additional interest because of suggestions that $V(CO)_5(\eta^3\text{-}H_3)$ might be stable.[51] In principle, such a species should be distinguishable from V-($CO)_5(\eta^2$-$H_2)$ by the frequency of its $\nu$(C–O) bands because of the change in oxidation state of the metal center.

When $V(CO)_6$ is irradiated with UV light in lXe solution *without* added reactants, two products are formed: one is short-lived, decaying rapidly after the lamp is switched off, while

(43) e.g.: Ishikawa, Y.; Brown, C. E.; Hackett, P. A.; Rayner, D. M. *Chem. Phys. Lett.* **1988**, *150*, 506.

(44) $PPh_3$ itself absorbe UV significantly at 308 nm. For our solutions, this absorption (ca. 50%) was measured by conventional UV spectroscopy. Before comparing the amount of $CpV(CO)_4$ destroyed, allowance was made for this UV absorption.

(45) PAC measurements are inherently more sensitive than TRIR, and our PAC cell has an optical path length of 1 cm, ca. 10 times longer than that of our standard TRIR cell. The result is that our PAC measurements were usually made with much lower concentrations of $CpV(CO)_4$ in the solution ($<10^{-5}$ M) than those used for TRIR (typically $7 \times 10^{-4}$ M). Under these dilute conditions, formation of dinuclear species[39] was negligible.

(46) See e.g.: Gonzalez, A. A.; Zhang, K.; Nolan, S. P.; Vega, R. L.; Mukherjee, S. L.; Hoff, C. D.; Kubas, G. J. *Organometallics* **1988**, *7*, 2429. Gonzalez, A. A.; Hoff, C. D. *Inorg. Chem.* **1989**, *28*, 4295.

(47) Shi, Q. Z.; Richmond, T. G.; Trogler, W. C.; Basolo, F. *J. Am. Chem. Soc.* **1984**, *106*, 71.

(48) Ishikawa, Y.; Hackett, P. A.; Rayner, D. M. *J. Am. Chem. Soc.* **1987**, *109*, 6644.

(49) (a) Perutz, R. N. Unpublished results. (b) Ford, T. A.; Huber, H.; Klotzbücher, W. E.; Moskovits, M.; Ozin, G. A. *Inorg. Chem.* **1976**, *15*, 1666. Hanlan, L.; Huber, H.; Ozin, G. A. *Inorg. Chem.* **1976**, *15*, 2592.

(50) For a more detailed account of these experiments, see refs 22b and 23b.

(51) Burdett, J. K.; Phillips, J. R.; Poliakoff, M.; Pourian, M.; Turner, J. J.; Upmacis, R. K. *Inorg. Chem.* **1987**, *26*, 3054.

**Table VIII.** Wavenumbers ($cm^{-1}$) of $V(CO)_6$ and Its Photoproducts in Liquid Xenon at ca. −70 °C and in *n*-Heptane and in the Gas Phase at Room Temperature

| species | lXe[a] | *n*-heptane[b] | gas phase[c] | assignment |
|---|---|---|---|---|
| $V(CO)_6$ | 1978[d] | 1975[d] | 1988 | $t_{1u}$ $\nu$(C–O) |
| $V(CO)_5(N_2)$ | 2219 | *f* | | $\nu$(N–N) |
| | 2075 | *f* | | $a_1$ $\nu$(C–O) |
| | 1955 | 1955 | | $a_1$ + e $\nu$(C–O) |
| $V(CO)_5(\eta^2\text{-}H_2)$ | 2080 | *f* | | $a_1$ $\nu$(C–O) |
| | 1955 | 1955 | | $a_1$ + e $\nu$(C–O) |
| $V(CO)_5(\eta^2\text{-}D_2)$ | 2076 | | | $a_1$ $\nu$(C–O) |
| | 1957 | | | $a_1$ + e $\nu$(C–O) |
| $V(CO)_5$ | 1944/1937[e] | 1942 | 1965 | $\nu$(C–O) |
| $V(CO)_4(N_2)_2$ | 2232 | | | $\nu$(N–N) |
| | 2215 | | | $\nu$(N–N) |
| | 2156 | | | $\nu$(N–N) |
| | 1922 | *g* | | $\nu$(C–O) |
| $V_2(CO)_{10}$[h] | 2080 | | | |
| | 2028 | | 2025 | |
| | 1960 | *i* | 1965 | |
| | 1890 | *i* | 1890 | |

[a] FTIR, ±0.5 $cm^{-1}$. [b] CO laser TRIR, ±2 $cm^{-1}$. [c] Reference 48. [d] Broad band. [e] Xe matrix, 20 K, from ref 49b. [f] Outside the wavenumber range of CO laser TRIR. [g] Secondary photolysis product, not observed by TRIR. [h] A shorter lived product, possibly $V_2(CO)_{11}$, was observed in lXe with $\nu$(C–O) bands at 2043, 2010, 2002, 1990, and 1951 $cm^{-1}$. [i] When TRIR was carried out under Ar (i.e. in the absence of added ligands), a broad partially resolved IR band was observed from 1960 to 1890 $cm^{-1}$.

the second longer lived product has $\nu$(C–O) bands close in wavenumber to those assigned to $V_2(CO)_{10}$ in the gas phase[48] (Table VIII). This behavior contrasts with that of $CpV(CO)_4$ (above), where irradiation in lXe in the absence of added ligands leads to only the weakest of the IR bands being assignable to dimeric species. When the experiment is repeated under a pressure of $N_2$ gas, a new product is observed with IR bands consistent with the formation of $V(CO)_5(N_2)$ (Table VIII). Further photolysis leads to the appearance of more $\nu$(N–N) bands, probably due to cis- and trans-$V(CO)_4(N_2)_2$. Similar sequential substitution of CO groups by $N_2$ has been observed previously for $Cr(CO)_6$ in lXe solution.[52] Again this contrasts with $CpV(CO)_4$, where substitution of more than one CO group by $N_2$ has not been observed in fluid solution. Even in the presence of $N_2$, the bands of the dinuclear vanadium species are still observed unless the starting concentration of $V(CO)_6$ in lXe is very low. In this respect, the behavior of $V(CO)_6$ is different from that of most, if not all, other carbonyl compounds which we have studied in lXe. Many of these other compounds have formed dinuclear species when irradiated in the absence of added ligands, but this process has been completely suppressed by addition of even modest pressures of $N_2$. The difference is probably the consequence of the odd electron configuration of the vanadium center in these species.

UV photolysis of $V(CO)_6$ in lXe in the presence of $H_2$ generates a new species with two $\nu$(C–O) bands close in wavenumbers to those of $V(CO)_5(N_2)$. The bands show modest shifts[53] when the experiment is repeated with $D_2$ (Table VIII). Venting the $H_2$ and subsequent repressurizing with $N_2$ leads to the disappearance of the new species and formation of $V(CO)_5(N_2)$. These observations are consistent with the formation of $V(CO)_5(\eta^2\text{-}H_2)$, but sadly, it was not possible to observe a $\nu$(H–H) band due to $\eta^2$-$H_2$. Such a band would only be observable with a relatively high concentration of $V(CO)_5(\eta^2\text{-}H_2)$ in solution. This could only be achieved with a high initial concentration of $V(CO)_6$, which leads to the formation of dinuclear species, see above. Nevertheless, the experiment provides clear evidence that the photochemical reaction of $V(CO)_6$ with $H_2$ does not involve oxidation of the metal center, since this would lead to a $\nu$(C–O) spectrum significantly different from that of $V(CO)_5(N_2)$.

TRIR experiments with $V(CO)_6$ in *n*-heptane solution at room temperature show that, as in lXe, the reactions with $N_2$ and $H_2$ lead to formation of $V(CO)_5(N_2)$ and $V(CO)_5(\eta^2\text{-}H_2)$ (Table VIII). Although thermal substitution reactions of $V(CO)_6$ normally occur associatively, the TRIR spectra show that the photochemical reaction proceeds via a short-lived $V(CO)_5$ intermediate (eq 8). The $\nu$(C–O) band of $V(CO)_5$ in *n*-heptane is in reasonable

$$V(CO)_6 \xrightarrow{UV,-CO} V(CO)_5 \xrightarrow{+L} V(CO)_5L \qquad (8)$$

agreement with the data from matrix isolation[49b] and gas-phase TRIR experiments[48] (Table VIII). TRIR traces for the reaction with $H_2$ are shown in Figure 15, and the bimolecular rate constants for reaction of $V(CO)_5$ with CO, $N_2$, and $H_2$ are given in Table IX. The following points are clear from these data: (i) $V(CO)_5(N_2)$ and $V(CO)_5(\eta^2\text{-}H_2)$ are both thermally more labile (Table IIB) than their $CpV(CO)_3L$ (Table IIA) or $Cr(CO)_5L$ analogs.[54] Such behavior is consistent with the thermal lability of $V(CO)_6$ itself. (ii) Like $CpV(CO)_3$ and $Cr(CO)_5$,[41] $V(CO)_5$ shows little

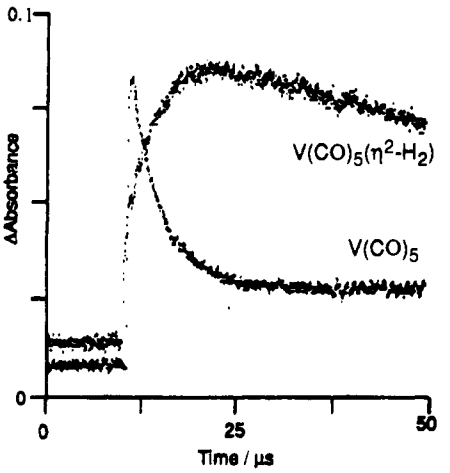


**Figure 15.** TRIR kinetic traces recorded during the UV flash photolysis of $V(CO)_6$ in *n*-heptane at room temperature under 2-atm pressure of $H_2$. Traces show the transient generation of $V(CO)_5$ and corresponding formation of $V(CO)_5(\eta^2\text{-}H_2)$. IR monitoring wavenumbers were 1942 $cm^{-1}$ for $V(CO)_5$ and 1955 $cm^{-1}$ for $V(CO)_5(\eta^2\text{-}H_2)$. Since there is some overlap between the absorption bands of the two species, the signal at 1942 $cm^{-1}$ does not return to zero absorbance, even after the reaction of $V(CO)_5$ is complete. This does not affect the kinetic analysis of the trace. Note that the reaction of $V(CO)_5$ is considerably slower than that of $CpV(CO)_3$ (Figure 14a).

**Table IX.** Rate Constants for the Pseudo-First-Order Thermal Decay of $V(CO)_5$ in *n*-Heptane at 25 °C

| L | [L]/mol $dm^{-3}$ | $k_{obs}/s^{-1}$ | $k_2$[a]/$M^{-1}$ $s^{-1}$ |
|---|---|---|---|
| Ar | | $2.9 \times 10^4$ | |
| CO | $2.4 \times 10^{-2}$ | $3.7 \times 10^5$ | $1.5 \times 10^7$ |
| $N_2$ | $4.8 \times 10^{-3}$ | $8.7 \times 10^4$ | $1.8 \times 10^7$ |
| | $1.9 \times 10^{-2}$ | $6.1 \times 10^5$ | $3.2 \times 10^7$ |
| $H_2$ | $2.3 \times 10^{-3}$ | $3.8 \times 10^4$ | $1.6 \times 10^7$ |
| | $9.0 \times 10^{-3}$ | $1.1 \times 10^5$ | $1.2 \times 10^7$ |

[a] $k_2$ calculated using the relationship $k_{obs} = k_2[L] + k_{Ar}$, where $k_{Ar}$ is the first-order constant for decay under 2-atm pressure of Ar in the *absence* of added ligands.

(52) Turner, J. J.; Simpson, M. B.; Poliakoff, M.; Maier, W. B., II; Graham, M. A. *Inorg. Chem.* **1983**, *22*, 911.

(53) The band assigned to the high-frequency $a_1$ vibration (ca. 2080 $cm^{-1}$) of $V(CO)_5(\eta^2\text{-}H_2)$ shows a shift to low wavenumber on deuteration. A reviewer has pointed out that this shift may indicate that the $\nu$(D–D) band, which we did not observe, is located to the high-wavenumber side of this $\nu$(C–O) band, implying that the corresponding $\nu$(H–H) band would be above ca. 2900 $cm^{-1}$ (i.e. $\sqrt{2} \times 2080$ $cm^{-1}$), significantly higher than the $\nu$(H–H) band of $CpV(CO)_3(\eta^2\text{-}H_2)$. The reviewer also commented that there is no shift in the corresponding $a_1$ $\nu$(C–O) bands of $Cr(CO)_5(\eta^2\text{-}H_2)$ and $Cr(CO)_5(\eta^2\text{-}D_2)$, but there, the $\nu$(D–D) band (2242 $cm^{-1}$) is quite far removed from the $\nu$(C–O) band (2090 $cm^{-1}$).

(54) (a) $Cr(CO)_5(N_2)$: Church, S. P.; Grevels, F.-W.; Hermann, H.; Schaffner, K. *Inorg. Chem.* **1984**, *23*, 3830. (b) $Cr(CO)_5(\eta^2\text{-}H_2)$: Church, S. P.; Grevels, F.-W.; Hermann, H.; Schaffner, K. *J. Chem. Soc., Chem. Commun.* **1985**, 30.

**Scheme I**

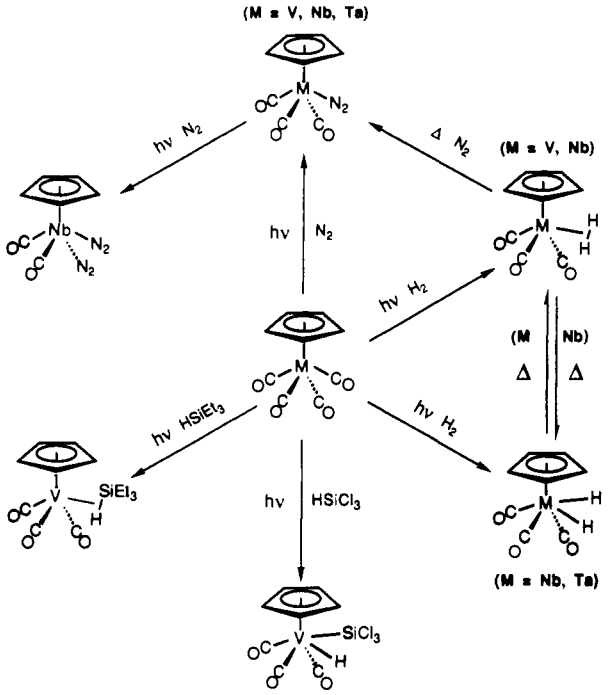


discrimination between incoming ligands; the rate constants for reaction with CO, $H_2$, and $N_2$ are very similar. (iii) $V(CO)_5$ is more reactive than $Cr(CO)_5$, but the difference in rate constants, about 1 order of magnitude, is smaller than might be expected from the enormous difference in reactivity between $V(CO)_6$ and $Cr(CO)_6$. (iv) $V(CO)_5$ is significantly less reactive than $CpV(CO)_3$; the rate constants in Table IX are almost exactly 10 times smaller than those of $CpV(CO)_3$ in Table VI. The implication of these observations is that, for ligands with relatively strong M–L interactions (e.g. CO, $N_2$, etc), the 18-electron $CpV(CO)_3L$ compounds have a greater thermal stability than the corresponding $V(CO)_5L$ species. With very weakly interacting ligands such as hydrocarbon solvents, some other factor destabilizes $CpV(CO)_3$···s relative to $V(CO)_5$···s. This factor is probably the steric bulk of the Cp ring, an effect similar to that which makes $Cp^*V(CO)_3$···s more reactive than $CpV(CO)_3$···s.

## Conclusions

This paper has described the spectroscopic characterization of a series of new compounds of V, Nb, and Ta. Scheme I contains the more important reactions revealed by our experiments. As in previous studies,[32] a combination of spectroscopic techniques has proved extremely fruitful; together the techniques are considerably more informative than individually. A particularly interesting observation is the similarity, both in kinetics and in energetics, between reactions which lead to oxidative addition and those which do not. Such addition reactions can be of considerable mechanistic importance, but in these group 5 compounds at least, the final outcome is extremely finely balanced.

The scheme is striking by the obvious parallels with reactions of $CpMn(CO)_3$ and $CpRe(CO)_3$. The difference, however, is that all of the group 5 compounds are thermally unstable and the intermediates more reactive than their group 7 counterparts. This reactivity merely continues a trend observed in the parent carbonyl compounds. For example $CpV(CO)_4$ undergoes reasonably facile thermal substitution reactions[37] while $CpMn(CO)_3$ does not. Indeed $Cp^*V(CO)_3$···(*n*-heptane) is one of the most reactive 16-electron intermediates so far detected by TRIR, ca. 5000 times more reactive toward $H_2$ than is $CpMn(CO)_2$···(*n*-heptane)[8] with a lifetime in solution shorter than that of some electronic excited states of organometallic compounds.[55]

Nevertheless, it is important to keep such differences in reactivity in perspective. If the kinetic behavior of these species were determined solely by the strength of the M···(*n*-heptane) interaction, the increased reactivity of $Cp^*V(CO)_3$···(*n*-heptane) could be produced by a V···(*n*-heptane) interaction which was only 21 kJ $mol^{-1}$ weaker than the Mn···(*n*-heptane) interaction. Although the behavior of the $CpMn(CO)_2$ fragment has been examined in some detail by the frontier molecular orbital approach,[56] it is difficult to treat $CpV(CO)_3$ in the same way; such calculations are very sensitive to variations in structure,[57] and no structural data are available for these systems. Qualitatively,[22b] the presence of a CO group trans to the coordination site in $CpV(CO)_3$ (**9**) will destabilize[22b] the $\pi$-donor orbital compared to that of $CpMn(CO)_2$ (**10**). However, this is probably little more than emphasizing that seven-coordinate compounds are generally more reactive than six-coordinate ones. Our observation of the greater reactivity of $CpV(CO)_3$ compared to $V(CO)_5$ provides additional support to steric arguments.

9

10

$CpMn(CO)_3$ has an extremely rich photochemistry[58] while the reactions of group 5 $CpM(CO)_4$ compounds are relatively unexplored. Our results indicate that further exploration in this area should be rewarding. In particular, the relative ease of polysubstitution of CO in $CpNb(CO)_3$ coupled with the rapid equilibrium between classical and nonclassical dihydrogen complexes suggests that this system might have potential catalytic activity, for example in the hydrogenation of dienes, similar to that observed with group 6 hexacarbonyl complexes.[32]

**Acknowledgment.** We thank SERC, the EC Science Program (Contract ST0007), NATO (Grant Nos. 900544/LG 920570), the Petroleum Research Fund administered by the American Chemical Society, the Paul Instrument Fund of the Royal Society, the British Council, Mütek GmbH, Perkin-Elmer Ltd., and BP International Ltd. for their financial support. We are particularly grateful to Ms. M. Jobling for carrying out the experiments in supercritical xenon described in this paper. We thank Professor M. Herberhold and F. Basolo for gifts of compounds critical to this work and Dr. A. J. Rest for his help and for providing data prior to publication.[14b] We are grateful to Professor V. N. Bagratashvili, Dr. P. M. Hodges, Dr. S. M. Howdle, Dr. S. A. Jackson, Professor O. Eisenstein, Professor R. N. Perutz, Professor U. Schubert, Professor N. Sheppard, Professor J. J. Turner, Professor E. Weitz, and Dr. A. H. Wright for their help and advice. Finally, we thank Mr. D. R. Dye, Mr. J. G. Gamble, Mr. D. Lichfield, Mr. R. Parsons, and Mr. J. M. Whalley for their continued assistance in developing and building the TRIR equipment at Nottingham.

(55) See e.g.: Glyn, P.; George, M. W.; Hodges, P. M.; Turner, J. J. *J. Chem. Soc., Chem. Commun.* **1989**, 1655.
(56) Rabaa, H.; Saillard, J.-Y.; Schubert, U. *J. Organomet. Chem.* **1987**, *330*, 397.
(57) See e.g.: Albright, T. A.; Burdett, J. K.; Whangbo, M. Y. *Orbital Interactions in Chemistry*; Wiley: New York, 1985.
(58) For a detailed review of the photochemistry of $CpMn(CO)_3$, see: Caulton, K. G. *Coord. Chem. Rev.* **1981**, *38*, 1.